**T.C.**
**ISTANBUL OKAN UNIVERSITY**
**INSTITUTE OF GRADUATE SCIENCES**

**THESIS**
**FOR THE DEGREE OF**
**MASTER OF SCIENCE**
**IN AUTOMOTIVE MECHATRONICS AND**
**INTELLIGENT VEHICLES PROGRAM**

**Kani Mudher Muhammed Ali KAKY**

# A COOPERATIVE POSITIONING METHOD FOR CONNECTED AND AUTOMATED VEHICLES

**THESIS ADVISOR**

Prof. Dr. Semih Bilgen

**ISTANBUL, April 2025**

**T.C.**
**ISTANBUL OKAN UNIVERSITY**
**INSTITUTE OF GRADUATE SCIENCES**

**THESIS**
**FOR THE DEGREE OF**
**MASTER OF SCIENCE**
**IN AUTOMOTIVE MECHATRONICS AND**
**INTELLIGENT VEHICLES PROGRAM**

**Kani Mudher Muhammed Ali KAKY**

**(203005013)**

# A COOPERATIVE POSITIONING METHOD FOR CONNECTED AND AUTOMATED VEHICLES

**THESIS ADVISOR**

Prof. Dr. Semih Bilgen

**ISTANBUL, April 2025**

**T.C.**

**ISTANBUL OKAN UNIVERSITY**

**INSTITUTE OF GRADUATE SCIENCES**

**THESIS**
**FOR THE DEGREE OF**
**MASTER OF SCIENCE**
**IN AUTOMOTIVE MECHATRONICS AND INTELLIGENT VEHICLES PROGRAM**

**Kani Mudher Muhammed Ali KAKI**

**(203005013)**

# A COOPERATIVE POSITIONING METHOD FOR CONNECTED AND AUTOMATED VEHICLES

Presentation Date of Thesis:

Submission Date of Thesis: March 25, 2025

Advisor: Prof. Dr. Semih Bilgen _____

Jury Members: Doç. Dr. Ömer Cihan Kivanç_____

Prof. Dr. Bekir Tevfik Akgün _____

# ACKNOWLEDGMENT

I express my sincerest gratitude to my supervisor, Professor Semih Bilgen, for his strong devotion and valuable reviews throughout my research journey. His unwavering dedication to achieving academic success and serious consideration of details have significantly shaped this thesis. Additionally, I'd like to thank everyone working at Okan University's Department of Automotive Mechatronics and Intelligent Vehicles for providing me with resources and support, which have been extremely beneficial in my journey.

# TABLE OF CONTENTS

# ABBREVIATIONS

| | |
|---|---|
| **A-GPS** | : Assisted-GPS |
| **BSM** | : Basic Security Message |
| **CAM** | : Class Awareness Message |
| **CVLC** | : Camera-based VLC |
| **DGPS** | : Differential GPS |
| **ETC** | : Electronic Toll Collection |
| **ETSI** | : European Telecommunications Standards Institute |
| **EKF** | : Extended Kalman Filters |
| **GIS** | : Geographic Information System |
| **GPS** | : Global Positioning System |
| **GOT** | : Grid-On-Road Localization |
| **HSP-VO** | : High-speed pavement visual odometry |
| **IMU** | : Inertial Measurement Unit |
| **INS** | : Inertial Navigation System |
| **IVCAL** | : Inter-Vehicle Communication-Assisted Localization |
| **KF** | : Kalman Filter |
| **LOS** | : Line of Sight |
| **LMICs** | : Low- and Middle-Income Countries |
| **MAE** | : Mean Absolute Error |
| **MAPE** | : Mean Absolute Percentage Error |
| **ML** | : Most extreme Probability |
| **OBU** | : On-Board Unit |
| **PLE** | : Path-Loss Exponent |
| **RF-GPS** | : Radiofrequency-GPS |
| **RSS** | : Received Signal Strength |
| **RSSI** | : Received signal-strength-indicator |
| **RSU** | : Roadside unit |
| **RMSE** | : Root Mean Square Error |
| **RMS** | : Root Mean Square |

| | |
|---|---|
| **RIALS** | : RSU/INS-aided localization system |
| **SDP** | : Semi-Definite Programming |
| **SINS** | : Strap-down inertial navigation system |
| **TDOA** | : Time difference of arrival |
| **TOA** | : Time of arrival |
| **UKF** | : Unscented Kalman Filter |
| **V2I** | : Vehicle-to-Infrastructure Communication |
| **V2R** | : Vehicle-to-Road Communication |
| **V2V** | : Vehicle-to-Vehicle Communication |
| **WLLS** | : Weighted Linear Least Squares |
| **3GPP** | : 3rd Generation Partnership Project |

# LIST OF TABLES

# LIST OF FIGURES

# ABSTRACT

A COOPERATIVE POSITIONING METHOD FOR CONNECTED AND AUTONOMOUS VEHICLES

This study investigates the ability of cellular-vehicle-to-anything (C-V2X) wireless communications to enhance AV localization in GNSS-deprived scenarios. Specifically, we propose CV2X-LOCA, a novel Road-Side-Unit (RSU)-assisted cooperative localization framework that leverages C-V2X channel state data to achieve lane-level accuracy. CV2X-LOCA includes four main components: a module of Information processing, an environmental parameter correction module, and a coarse positioning module and the vehicle trajectory filtering module collectively address challenges in dynamic C-V2X networks. The vehicle localization model in general demonstrates that CV2X-LOCA attains cutting-edge localization performance even in noisy conditions, with fast-moving vehicles and sparse RSU coverage. The findings provide transportation agencies with valuable insights to help them make informed decisions regarding the future cost-effective deployment of RSUs.

**Keywords**: localization system, cellular-vehicle-to-everything, RSU, navigation satellite systems.

# ÖZET

## BAĞLANTILI VE OTONOM İŞBIRLIKÇI KONUMLANDIRMA

ÖZET - Otonom araçların güvenli bir şekilde şehir ortamlarında seyir yapabilmeleri için kesin ve dayanıklı bir konumlandırma sistemi esastır. Mevcut yöntemler genel navigasyon uydu sistemlerine (GNSS) dayandığı zaman açık alanlarda etkili olsa da, çok katlı köprülerin alt katları, yüksek binalarla çevrili yollar ve metro gibi şehir kanyonlarında hassas konum belirleme zorlukları devam etmektedir. Bu çalışma, GNSS'den yoksun senaryolarda C-V2X kablosuz iletişimin otonom araç konumlandırmasını nasıl geliştirebileceğini araştırmaktadır. Özellikle, sadece C-V2X kanal durumu verilerini kullanarak şerit düzeyinde hassasiyet elde etmek için RSU destekli işbirlikçi bir konumlandırma alt yapısı olan CV2X-LOCA'yı öneriyoruz. CV2X-LOCA, bilgi işleme modülü, çevre parametre düzeltme modülü, kaba konumlandırma modülü ve araç izdüşümü filtreleme modülünden oluşan dört ana bileşeni içermekte olup, dinamik C-V2X ağlarındaki zorluklara kolektif olarak yanıt vermektedir. Genel modelleme, CV2X-LOCA'nın gürültülü koşullarda, hızlı hareket eden araçlar ve seyrek RSU kapsamında dahi son teknoloji konumlandırma performansı elde ettiğini göstermektedir. Bulgular, ulaşım kurumlarının gelecekte maliyet etkin RSU dağıtımına ilişkin bilinçli kararlar almasına değerli içgörüler sunmaktadır.

**Anahtar kelimeler**: Sistem Yerelleştirme, Hücresel-Araç-Herşeye, RSU, Navigasyon Uydu Sistemleri.

# CHAPTER 1. INTRODUCTION

## 1.1. PROBLEM STATEMENT

Each year, approximately 1.3 million people die every year as a result of street activity accidents. Furthermore, street activity crashes result in genuine wounds for 20 to 50 million individuals each year. Street activity accidents have devastating financial and mental impacts on casualties, families, communities, and nations. The financial impact comes from the cost of therapeutic care, the misfortune of compensation for individuals murdered or rendered debilitated by their wounds, and caregiving costs for family members who must take time off work or school to look after the harmed. In any case, low- and middle-income countries (LMICs) have the most prominent burden of traffic hazards.

To enhance traffic safety and accident prevention systems, effective vehicle localization strategies are essential. Recent advancements have led to the development of various localization techniques, broadly categorized into relative and absolute positioning methods. Absolute positioning relies on technologies such as Road-Side Units (RSUs) or the Global Positioning System (GPS) to determine a vehicle's location independently. However, these methods often lack the precision required for accident prevention applications, mainly due to their low accuracy and limited availability.

Alternatively, relative positioning techniques utilize intervehicle communication and cooperative methods to establish the positions of vehicles relative to each other. Despite their potential, these methods face challenges such as limited sensor range, high sensor costs, issues with hidden vehicles, and reduced accuracy in adverse weather conditions [1].

This study aims to guide transportation agencies' future investment decisions regarding cost-effective RSU deployment. Unlike existing methods that rely on multiple RSUs for localization, our framework enables each vehicle to determine its

location relative to a single RSU, significantly reducing setup costs. However, this approach introduces challenges in achieving high-precision vehicle localization.

Our proposed framework comprises four stages:

1. Defining the driving direction of vehicles.
2. Using Received signal-strength (RSS) ranging to measure the gap between the vehicle and the RSU.
3. Refining the vehicle's position using Kalman filters and inertial navigation system data.
4. Ensuring the vehicle's position remains within road boundaries.

Simulation results demonstrate that our single-RSU localization framework outperforms both GPS-based and existing RSU-based methods in terms of precision, with localization errors of less than 1.8 meters. The increase in precision compared to GPS-based methods is up to 65%, and compared to existing RSU-based methods, it reaches approximately 73.3%.

## 1.2. AIM and OBJECTIVE of the STUDY

The main purpose of this study is to enhance the localization accuracy of autonomous vehicles by utilizing Road-Side Units (RSUs) in combination with the vehicles' onboard sensors and systems. Our work has the following objectives:

- **Enhanced Localization Precision:**

  By leveraging RSUs, which are fixed infrastructure units installed along roadways, the system seeks to improve the precision of vehicle localization beyond what can be achieved using onboard sensors alone, such as GPS, Inertial Measurement Units (IMUs), or cameras.

- **Improved System Robustness in Challenging Conditions:**

  Autonomous vehicles often face challenges such as GPS signal loss in urban

canyons or adverse weather conditions. The system aims to mitigate these challenges by integrating RSUs, which can provide supplementary positioning information even in GPS-denied environments or under unfavorable weather conditions.

- **Increased Reliability and Safety:**

  Reliable and accurate localization is crucial for the safe operation of autonomous vehicles. By incorporating RSUs into the localization system, the objective is to enhance the reliability of vehicle positioning, thereby improving overall safety for passengers, pedestrians, and other road users.

- **Real-Time Updates and Corrections:**

  RSUs can offer real-time updates and corrections to vehicles' position estimates, allowing for dynamic adjustments in navigation and control algorithms. This capability is particularly valuable in scenarios where road conditions change rapidly, such as in construction zones or during accidents.

- **Adaptability and Interoperability:**

  The system aims to be adaptable across different road networks and compatible with various autonomous vehicle platforms. It seeks to establish standards and protocols for communication between RSUs and vehicles to ensure interoperability and seamless integration into existing transportation infrastructure.

-

## 1.3. OUTLINE of the THESIS

The thesis is organized as follows:

- **Chapter 1: Introduction:**
  The thesis begins with an introduction that provides a brief overview of vehicle localization and outlines the aim of the study.

- **Chapter 2: Literature Review:**

  This chapter presents an extensive review of the relevant literature, exploring existing research and developments in the field of vehicle localization.

- **Chapter 3: Theory and Methodology:**
  The theoretical framework and methodology employed in this study are detailed in this chapter, explaining the approaches and techniques used to achieve the research objectives.

- **Chapter 4: Simulation Model and Results:**
  This chapter clarifies the simulation model developed for the study and presents the results obtained from the simulations.

- **Chapter 5: Conclusion:**
  The final chapter provides a summary of the key achievements of the study, compares the results with recent similar efforts, and evaluates the limitations of the current work. It ends in a short review of possible areas for further research.

# CHAPTER 2. RELATED WORK

This chapter will examine recent advancements in vehicle localization and its related fields, organized into four primary categories:

- **Passive Localization:**
  This category includes methods that rely on GPS, navigation sensors, and other sources not directly influenced by environmental factors.
- **Map Matching:**
  In this approach, localization accuracy is enhanced by incorporating an understanding of the surrounding environmental context.
- **Vision-Based Localization:**
  This category involves using sensors to observe and interpret the vehicle's surrounding environment for localization purposes.
- **Data Association:**
  This involves identifying and associating detected objects, which is crucial for overcoming challenges in both vision-based localization and map matching.

✓ Passive Localization

Passive localization methods rely on vehicle motion measurements, utilizing the last known position, direction, and speed. These methods employ various sensors, including odometers, accelerometers, compasses, and gyroscopes. Information sources such as GPS, Inertial Navigation Systems (INS), and other dead reckoning sensors like wheel-speed sensors and compasses are integrated to create a robust localization framework. Dead reckoning provides relative changes in the vehicle's location when GPS signals are unreliable, while GPS offers reference positions for calibration. Most approaches use Kalman Filters (KF) or Extended Kalman Filters (EKF) for localization, adjusting their application based on the specific method employed [2].

✓ Map Matching

Map matching, a fundamental component of localization systems, involves identifying the road the vehicle is traveling on and adjusting the estimated vehicle position accordingly. Taylor's method matches raw GPS points to nearby road shapes, filtering out significantly different roads and refining position estimates through a least-squares model. While map matching primarily improves lateral position estimation, additional information, such as changes in vehicle direction or landmarks, contributes to the refinement of longitudinal positioning [3].

✓ Vision-based Localization

Vision-Based Localization integrates position and heading estimates from detailed road maps with GPS-dead reckoning systems, utilizing Kalman or particle filters. As demonstrated by Chausse, this method extends to multi-lane roads, emphasizing the reduction of uncertainty in lateral positioning [4]. Other researchers, such as Georgiev and Allen, incorporate vision along with GPS and dead reckoning for urban robotic pose estimation. They enhance localization precision by leveraging detectable urban features that are mapped within Geographic Information System (GIS) databases [5].

✓ Data Association

Data association involves linking position measurements to the corresponding entities being measured, which can be challenging in dynamic environments. Failure to accurately associate these measurements can lead to significant inaccuracies in the vehicle's position estimates. Therefore, effective data association strategies are crucial for ensuring precise localization and minimizing the biases introduced by incorrect associations [6].

[7] paper explores the potential of cellular-vehicle-to-everything (C-V2X) communications to enhance autonomous vehicle (AV) localization in GNSS-denied environments. They introduce CV2X-LOCA, the first cooperative localization framework leveraging roadside units (RSUs) and C-V2X channel state information to

achieve lane-level positioning accuracy. CV2X-LOCA comprises four key components: a data processing module, a coarse positioning module, an environment parameter correction module, and a vehicle trajectory filtering module, each addressing challenges in dynamic C-V2X networks. Extensive simulations and field tests confirm CV2X-LOCA's state-of-the-art performance for vehicle localization, even in high-speed, noisy, and sparse RSU environments. Although designed for AV localization, CV2X-LOCA's applications can extend to other C-V2X-enabled road users. These findings offer valuable insights for transportation agencies on cost-effective RSU deployment strategies.

[8] explained that current AV sensor systems provide significant benefits in V2V and V2I contexts, with features like blind spot coverage, extended range, and weather resilience; however, they primarily focus on vehicle-to-vehicle communication. Vulnerable Road User (VRU) identification presents unique challenges, including localization obstacles, limited communication capabilities, and as well as network accessibility gaps. This review evaluates the latest advancements in V2X and AV technologies, proposing an end-to-end AV motion control framework with a temporal deep learning method that models dynamic actions of both visible and non-line-of-sight (NLOS) traffic users. It also assesses various AI solutions to enhance VRU identification, tracking, and communication.

Also recently, [9], proposed an integrated sensing and communication (ISAC) system Utilizing cellular vehicle-to-everything (C-V2X). Initially, [9] assess the viability of using the new radio (NR) waveform within the ISAC framework, exploring its potential for sensing based on NR-V2X standards. They calculate the ambiguity function to determine the sensing efficiency limits of the NR waveform. A C-V2X-based ISAC system is then designed to simultaneously support communication and sensing in vehicular networks. They present an integrated structure that combines vehicular communication with automotive sensing using the existing NR-V2X network. Using ISAC framework, the work develops a receiver algorithm for target recognition and estimation, alongside communication, with minimal adjustments. Performance evaluations of the proposed ISAC system demonstrate highly reliable

communication, achieving 99.9999% throughput, and precise sensing, with faults under 1 meter and 1 m/s in vehicle scenarios.

[10] presented a multi-modal vehicle positioning framework that combines channel state information (CSI) with images to jointly localize vehicles. The approach targets outdoor environments where each vehicle communicates with a single base station (BS) and uploads its estimated CSI to that BS. Each BS is equipped with cameras, enabling the collection of a small set of labeled CSI data, a large volume of unlabeled CSI, and corresponding images. To leverage the unlabeled CSI data and image-derived position labels, a meta-learning-based hard expectation-maximization (EM) algorithm is developed. Given the unknown correspondence between unlabeled CSI data and multiple vehicle positions in images, the training objective is formulated as a minimum matching problem. A weighted loss function is applied to mitigate label noise caused by mismatches between unlabeled CSI and vehicle positions, enhancing convergence. A meta-learning algorithm is then used to calculate the weighted loss, which updates model parameters based on the unlabeled CSI samples and their matched position labels. Simulations demonstrate that this approach reduces positioning error by up to 61% compared to methods relying solely on CSI fingerprints for vehicle positioning.

[11] presented a fusion strategy combining ultra-wideband (UWB) technology with onboard sensors to achieve precise and reliable vehicle positioning. The approach involves a two-step process: preprocessing UWB measurements and globally estimating vehicle position. Initially, an ARIMA–GARCH model is developed to address the non-line-of-sight (NLOS) issue in UWB under vehicular traffic conditions, allowing for efficient detection and correction of NLOS errors. Subsequently, an adaptive interacting multiple model (AIMM) algorithm is introduced for global fusion, enhancing positioning accuracy by dynamically adjusting model probabilities to align with current driving conditions. The method’s effectiveness and feasibility are confirmed through field tests, which demonstrate improved positioning accuracy compared to traditional IMM approaches.

[12] explained that accurate positioning is essential for deploying Connected Automated Vehicles (CAVs). A growing trend is the use of cooperative techniques, in which vehicles integrate data from navigation and imaging sensors for joint positioning and environmental awareness. This research introduces a data-driven cooperative sensing framework, Cooperative LiDAR Sensing with Message Passing Neural Network (CLS-MPNN), where vehicles communicate to perceive their surroundings using LiDAR sensors. Evaluations in two realistic driving scenarios produced by a high-quality simulator show that CLS-MPNN outperforms traditional non-cooperative GNSS-based localization and a leading cooperative SLAM method, getting closer to the accuracy of an idealized system with perfect sensing and data association.

## 2.1. ABSOLUTE POSITIONING METHODS

### 2.1.1. Absolute Positioning Based on GPS

This localization method utilizes the Global Positioning System (GPS) to determine the location of each vehicle. Typically, GPS localization methods involve GPS receivers continuously receiving data transmitted by GPS satellites. Using a method known as Time of Arrival (TOA), these methods approximate the vehicle's distance from at least 4 identified satellites, followed by the computation of the actual position through trilateration. However, GPS-based methods face several challenges. A significant issue is the inherent low precision of GPS systems, typically ranging between 10 to 30 meters, which is inadequate for effective vehicle collision warning systems. As a result, several enhancements to basic GPS methods have been proposed to improve localization precision. One such method is Radio Frequency-GPS (RF-GPS), which utilizes a concept called Differential GPS (DGPS) to refine GPS precision. DGPS involves using multiple reference stations at known positions, each provided with GPS receivers, to calculate and broadcast error corrections. Additionally, GPS-based methods encounter difficulties in urban environments where tall buildings obstruct the satellite signals received by vehicle GPS receivers. Assisted-GPS (A-GPS) has been introduced to enhance typical GPS performance in cellular network-connected

devices by utilizing an A-GPS server. Despite the availability of enhanced GPS versions like A-GPS and RF-GPS, their implementation requires additional infrastructure, thereby increasing costs [13] [14].

### 2.1.2. GPS-Free Absolute Positioning

The need for GPS-free localization methods arises due to the limitations of GPS positioning algorithms, which typically exhibit a localization error ranging between 10 and 30 meters, making them unsuitable for collision warning systems. In response, innovative methods leveraging Road-Side Units (RSUs) have been introduced to overcome the reliance on GPS methods. RSUs are strategically placed along roadsides, with all vehicles supplied with Onboard Unit (OBU) devices capable of communicating with these RSUs. Consequently, each vehicle can approximate its position relative to the RSUs [15].

One proposed method, as outlined in [16], involves the installation of two RSUs on each side of the road, with each vehicle estimating its location relative to these RSUs using a method called "faulty free." Additionally, [16] explores scenarios where one RSU may malfunction, termed "faulty," leaving only one RSU operational. Alternatively, the technique outlined in [17] relies on initial position determination using information from a single RSU, followed by updating the position using dead reckoning. Dead reckoning, originally employed in GPS-based methods to address GPS coverage gaps, serves as an effective substitute to inter-vehicle communication methods. However, the accumulation of dead reckoning errors leads to significant deterioration in localization precision over distance, as demonstrated in simulation results.

In contrast to the approach in [17], which does not utilize position-measuring methods such as TOA, Received Signal Strength (RSS), or Time Difference of Arrival (TDOA), the researchers in [18] propose employing TOA-based distance measurement to mitigate positioning errors. This strategy aims to limit the use of faulty dead reckoning to the vicinity of the RSU, thereby enhancing localization precision.

Additionally, to enhance predictability and precision in vehicle localization, numerous studies have developed cooperative localization methods that operate without GPS [19]. One such method employs a three-step process. Initially, each vehicle estimates distances to its surrounding entities using the Received Signal Strength Indicator (RSSI). This information is then shared with nearby vehicles, allowing each vehicle to refine its position estimates using Kalman filters, taking into account vehicle kinematics and road constraints. This procedure is repeated periodically to keep the vehicle's position estimation current.

GPS-based localization methods often face challenges that reduce accuracy, such as signal reflections (multipath) and obstructions from tall buildings or tunnels. Unlike these methods, our proposed localization system uses RSUs for localization. This approach not only enhances accuracy but also simplifies the existing node localization algorithms. We further improve localization accuracy by integrating relative positioning techniques. Importantly, our system relies solely on the vehicle’s own data, without the need for inter-vehicle communication.

## 2.2. RELATIVE POSITIONING METHODS

None of the mentioned absolute localization methods are appropriate for collision avoidance applications because of their limited precision. Moreover, these methods lack the capability to determine the vehicle's path of travel, making them insufficient for collision avoidance systems that depend on precise knowledge of relative distances between vehicles. In response to these limitations, relative positioning techniques have been developed to enhance positioning precision by facilitating the exchange of location information between vehicles, enabling them to collaboratively achieve more accurate positioning relative to each other.

These cooperative approaches, as described in [20], involve estimating inter-vehicle distances through various means such as RSSI, TOA, a combination of RSSI and two-way TOA, vision-based sensors, millimeter-wave radar sensors, or Doppler shift. By employing these inter-vehicle range techniques, vehicles can accurately

determine their positions relative to neighboring vehicles, thereby improving overall positioning accuracy and enhancing collision avoidance capabilities.

### 2.2.1. Relative Positioning Based on GPS

Many current relative positioning strategies incorporate GPS data as an input to the positioning algorithm. The Inter-Vehicle Communication-Assisted Localization (IVCAL) technique employs a Kalman Filter (KF) to combine localization data gathered from both the Inertial Navigation System (INS) and GPS. The location obtained from the KF, along with the relative distance prediction derived from inter-vehicle communication, is combined using least-squares optimization to improve the positioning precision of each vehicle within the network [21].

Similarly, the Grid-On-Road Localization (GOT) system was designed to utilize vehicle cooperation, allowing vehicles in GPS-challenged environments, such as subways or roads surrounded by tall buildings, to precisely determine their positions. This is accomplished through collaboration with a minimum of three vehicles equipped with reliable GPS signals, utilizing the estimation of inter-vehicle distance [22].

### 2.2.2. GPS-Free Relative Positioning

To enhance predictability and increase precision in vehicle localization, numerous GPS-free cooperative vehicle localization methods have been developed, eliminating reliance on GPS assistance. For example, [23]introduced a three-phase localization method where each vehicle initially approximates inter-vehicle distances using RSSI. Subsequently, vehicles share this information with neighbors, refining their estimations alongside vehicle kinematics and road constraints utilizing Kalman filters. This iterative process ensures continuous updates of vehicle positions. Meanwhile, [24] proposed a two-phase GPS-free neighbor-vehicle mapping framework. Here, vehicles acquire status of surrounding vehicles being present or not, via vision-based environment sensors covering specific calibrated regions. After exchanging status information, vehicles construct relative local maps linking neighbors' data with their communication addresses (e.g., MAC/IP) and their relative positions.

GPS-based positioning methods encounter various issues, such as multipath interference and signal obstruction in urban environments or subways. In contrast, our designed localization technique relies on RSUs for localization, aiming to enhance precision and algorithmic simplicity. Additionally, we leverage fusion methods developed for relative positioning to further improve localization precision. Our approach solely relies on each vehicle's own data without the need for inter-vehicle data exchange.

## 2.3. SOME RELATED WORK RESULTS

In this section, two different localization methods will be presented and discussed. These methods represent distinct approaches to localization, each contributing to an independent field of position determination and both differing from the algorithm proposed in this work.

Guowei Wan and Xiaolong Yang [25], in their paper titled "Enhancing Vehicle Localization Precision and Reliability through Multi-Sensor Fusion in Varied Urban Environments," devised a system that dynamically integrates data from multiple related sensors such as LiDAR, GNSS, and IMU to achieve superior positioning precision and flexibility in challenging environments, including urban centers, highways, and subways. Instead of relying solely on LiDAR intensity or 3D geometry, their approach ingeniously incorporates both LiDAR intensity and altitude cues, highly improving the precision and robustness of the localization system. The GNSS RTK module benefits from the multi-sensor fusion framework, leading to improved success rates in resolving ambiguities. An error-state Kalman filter is employed to merge position measurements from diverse sources, utilizing a novel uncertainty estimation method. The study extensively validates the effectiveness of the proposed methodologies, achieving a Root

Mean Square (RMS) precision of 5-10 cm, thereby surpassing the efficiency of prior state-of-the-art systems.

Figure 2.1 shows the structure of multi-sensor fusion substructure.

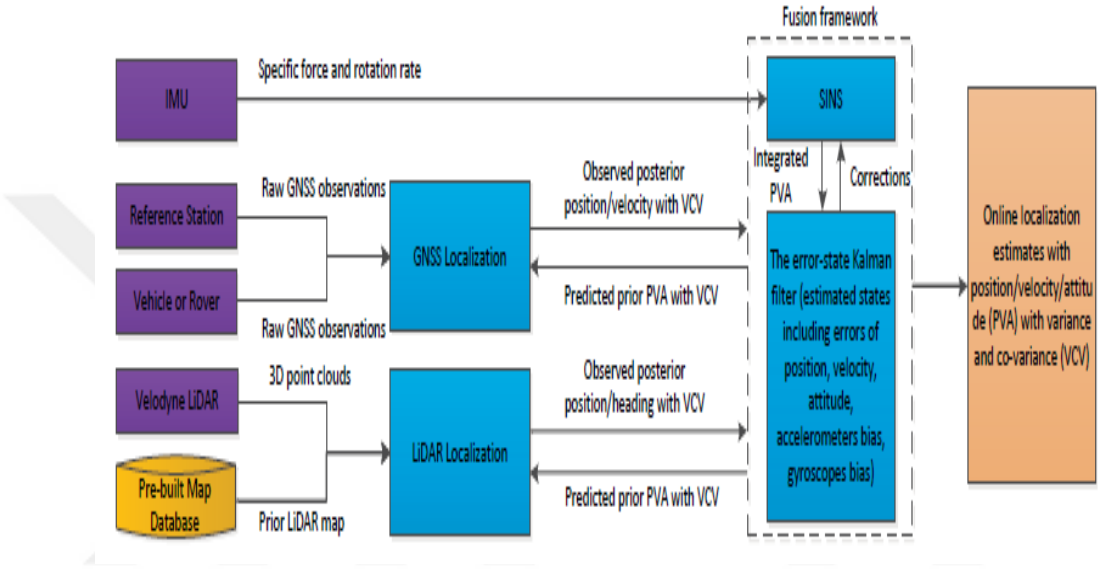


Figure 2.1. The structure of the method proposed in [25].

The system integrates sensor inputs (depicted in purple) with a pre-built LiDAR map (depicted in yellow) to approximate the optimum location, speed, and attitude (PVA) of the autonomous vehicle. GNSS and LiDAR provide measurements for the PVA, which are utilized by an error-state Kalman filter to generate the predicted prior PVA. In the Kalman filter's propagation phase, the strap-down inertial navigation system (SINS) serves as an expectation model by incorporating the specific force $f_b$ defined by the accelerometer and the rotation rate $w_b^{ib}$ defined by the gyroscope. Adjustments containing gyroscope and accelerometer biases and PVA errors, valued by the KF, are supplied back to the SINS.

In the LiDAR-based module localization, the system jointly approximates location, speed, and attitude (PVA). In addition, it employs an optimal solution focusing solely on the 3-dimensional location and the heading, denoted as (x, y, a, h). The algorithmic details are illustrated in Figure 2.2.

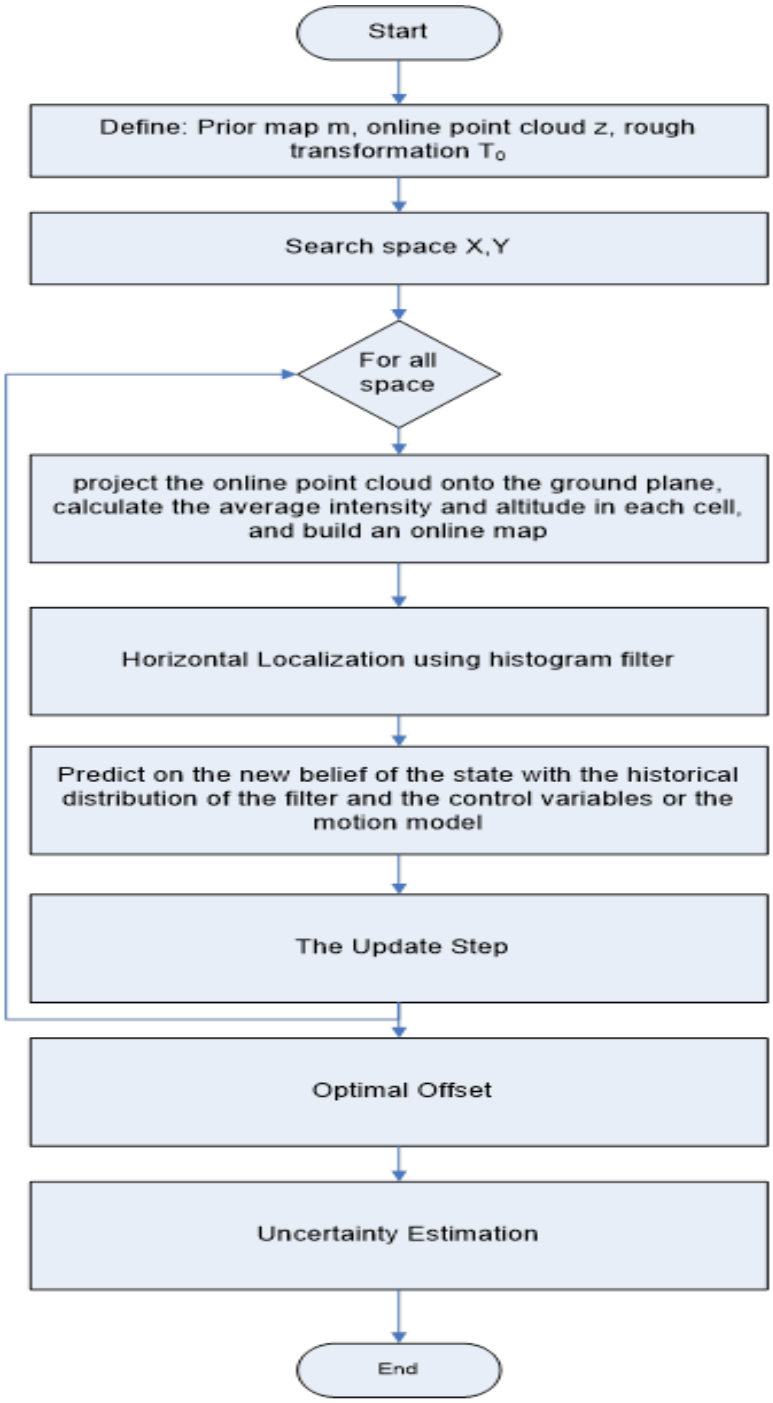


Figure 2.2. Algorithm flow chart presented in [25].

The system developed in that study dynamically combines input from sensors that are complementary, like GNSS, IMU, and LiDAR, to attain accurate positioning in diverse and demanding environments such as urban center areas, highways, expressways, and subways. It achieves impressive Root Mean Square (RMS) accuracies of 5-10 cm both laterally and longitudinally, rendering it suitable for industrial deployment. The versatility of the paper fusion substructure and algorithm design enables easy integration of additional sensors at varying cost levels to address different application needs.

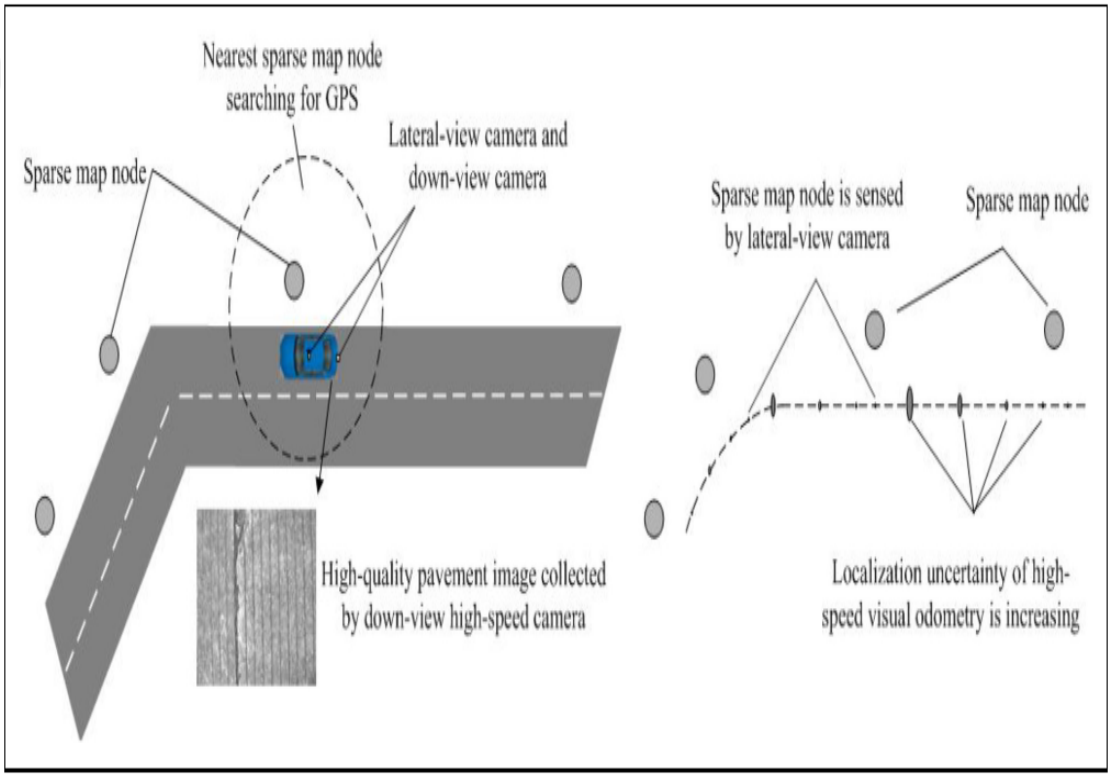


Figure 2.3. Illustration of the proposed method in [26].

Huang, Gang, et al. [26] developed an improved method for smart vehicle self-positioning by integrating a sparse visual map and large-velocity pavement visual odometry. The smart vehicle in their study is controlled by a GPS receiver, a lateral-view camera, and a down-view camera, as depicted in Figure 2.3. The proposed method comprises two main steps.

First of all, a sparse visual map is generated. Subsequently, using an in-vehicle GPS, a lateral-view camera, and a down-view camera, the vehicle localization is computed. Specifically, the localization process involves three key components:

- Searching for the nearest sparse map node using GPS.
- Localization is based on sparse map nodes, utilizing the lateral-view camera.
- High-speed pavement visual odometry (HSP-VO) using the down-view camera. This high-speed camera maintains consistent imaging resolution of pavement features, even at high speeds.

Figure 2.4 depicts the proposed method.

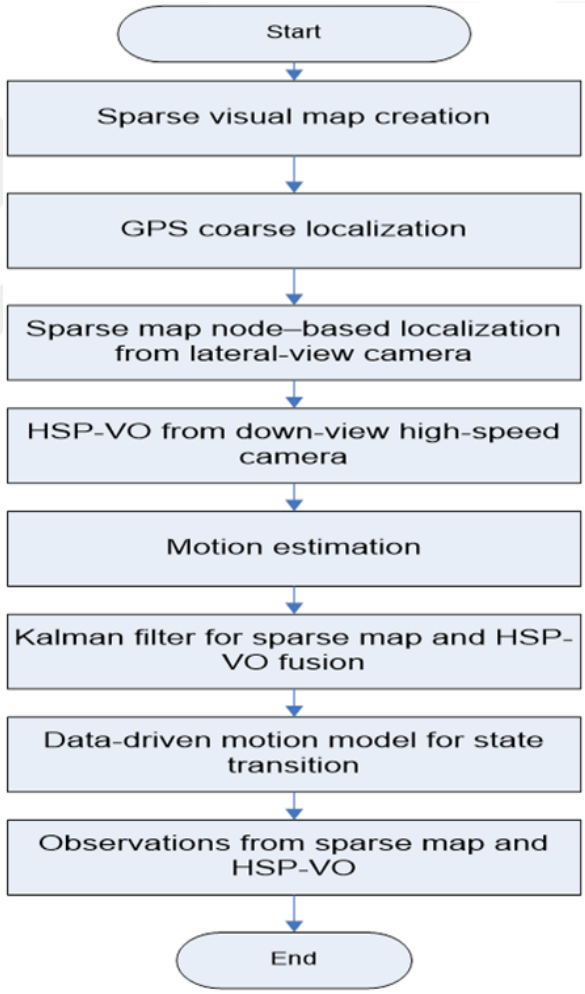


Figure 2.4. Flow chart for the method proposed in [26].

Having discussed the previous algorithms, the next chapter will present the theoretical principles underlying the algorithm used in our localization process. The

proposed algorithm employs different parameters from those used in the two previously discussed algorithms.

# CHAPTER 3. THEORY AND METHODOLOGY

## 3.1. THEORY

### 3.1.1. GPS-free Localization Techniques

The main task of a sensor network is to gather and transmit information to its target. It’s crucial to be aware of the location of the data that has been collected. This type of data can be found by localization techniques in wireless sensor networks (WSNs). Localization is a method for calculating the position of sensor nodes. The localization of sensor nodes is a promising study domain, with numerous studies published to date.

GPS-based systems are too expensive due to the need to install a GPS receiver on each node, despite the fact that localization accuracy is quite excellent. GPS-free methods do not utilize GPS, and they compute the distance among the nodes related to the local network, they are less expensive than GPS-based systems as well. A number of nodes require localization via GPS, referred to as anchor or beacon nodes, which begin the localization procedure.

**Range-free methods**: Utilize radio connectivity to enable communication among nodes to determine their locations. Some of these methods are distance vector (DV) hop, hop terrain, and centroid system. In range-free strategies, distance measurement, angle of arrival, and advanced equipment are not required.

**DV Hop:** This method predicts the range among nodes based on hop count. A minimum of three anchor nodes transmit coordinates together with hop count throughout the network.

**Hop Terrain:** Hop terrain is identical to DV hop approach in determining anchor node's distance from unlocalized node.

**Range-Based Localization**

**Received Signal Strength Indication (RSSI)**: In RSSI, the distance between the receiver and the transmitter is determined by evaluating the signal quality at the reception. Propagation loss is also determined, and it is transformed into distance estimation.

**Time of Arrival (TOA):** In (TOA), the velocity of wavelength and the duration of radio signals transmitted between the anchor node and the unlocalized node are determined in order to identify the position of the unlocalized node. GPS apply TOA, and it is an extremely accurate method; however, it needs significant processing power.

We obtained remarkable results through the comparison of several localization strategies.

Figure 3.1illustrates the costs of four localization methods, revealing that GPS- and TOA-based systems are more costly than DV hop and RSSI methods.

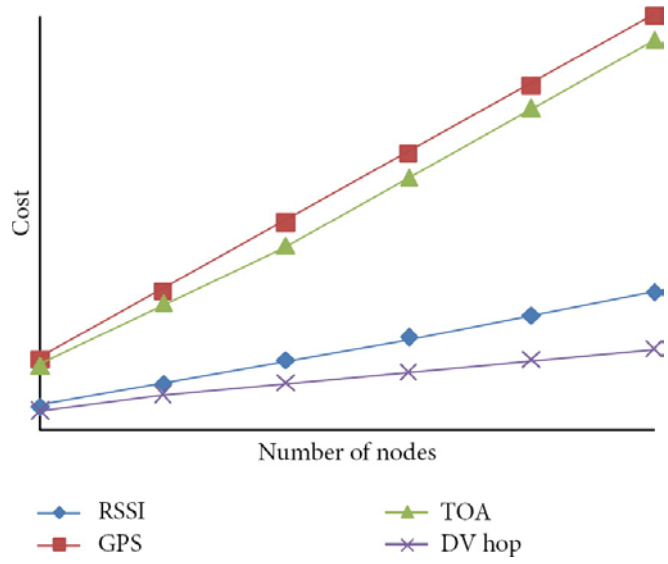


Figure 3.1. Cost analysis of localization techniques.

Such methods are essential for WSNs, which are saving energy. Figure 3.2 shows analysis of energy conservation of several localization methods. GPS-based localization techniques exhibit lower energy efficiency whereas RSSI-based methods demonstrate high energy efficiency.

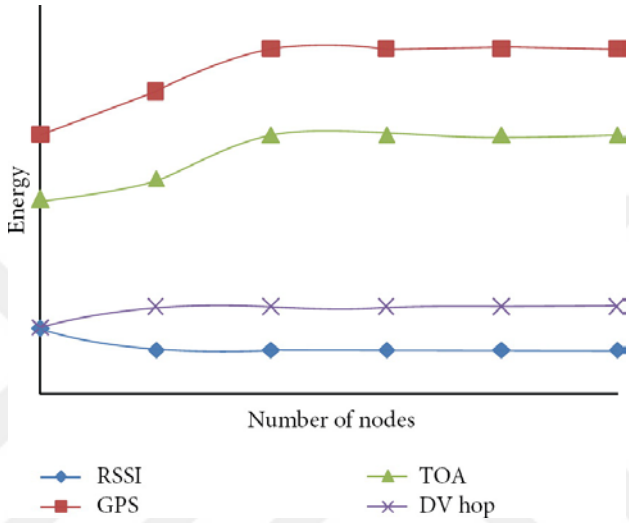


Figure 3.2. Energy efficiency analysis of different localization methods.

In our system, vehicle localization does not rely on GPS receivers. Instead, each vehicle is provided with onboard unit (OBU) devices for evaluating the distance of the vehicle from Road-Side Units (RSUs) through vehicle-to-road (V2R) communication. We utilize direct communication links with the PC5 interface operating at 5.9 GHz, as specified by 3GPP for intelligent transportation systems. RSUs are installed on only one side of the road and periodically broadcast beacons that include the road ID and the RSU's location. While neighboring vehicles share their positions for collision avoidance via vehicle-to-vehicle (V2V) communication, V2V is not used in the localization process itself and is therefore outside the scope of this paper.

Each vehicle is supplied with standard devices such as a digital odometer, a compass, and an Inertial Navigation System (INS). The INS is a navigation method that computes the current position in relation to a prior one by measuring the vehicle's

velocity and orientation. This system typically uses accelerometers to capture velocity data and gyroscopes to determine direction.

We suppose that vehicles travel on a dual carriageway road divided by Reservations made centrally. The road is linear entirely, with multiple entry and exit points. This type of road model is commonly used in related studies. Every entry point is supplied with an RSU. We assume that this entry and exit points are staggered, meaning that at any given y-coordinate, there is an entry on one side of the road and an exit on the opposite side, as illustrated in Figure 3.3. The road includes shoulders that vehicles can use to change their driving direction but has no intersections. We also assume that the distance between the vehicle and the RSU (R) is significant, the road's width (W) is relatively small compared to its length (L), and thus, the road's curvature can be considered nearly linear.

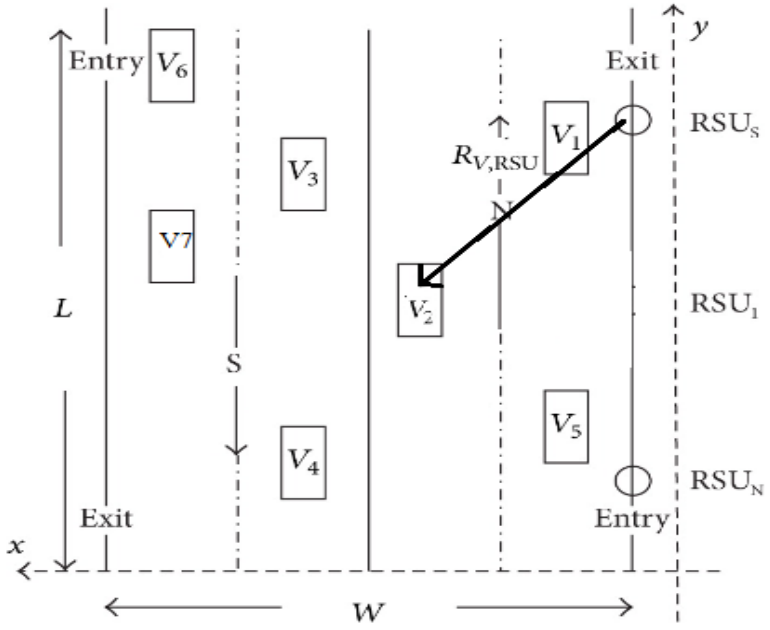


Figure 3.3. System model.

## 3.1.2. Determining the Vehicle Driving Direction

This section outlines our proposed method for determining the driving direction. Previous approaches, such as the one described in [14], suggest using two RSUs placed on either side of the road. In that method, a vehicle identifies its driving direction by

comparing the angle of its current movement vector with the direction to the north or south RSU. Another method involves RSUs installed on only one side of the road, where a vehicle must receive and analyze position information from two consecutive RSUs to ascertain its direction.

In our system, the primary challenge is determining the driving direction using only one RSU on a single side of the road while also minimizing start-up time. To address this, we suggest the next algorithm, which is activated each time a vehicle enters a new road segment to determine its direction of travel. For simplicity, we designate travel direction to be either north (N) or south (S). However, the exact travel direction is derived by interpolating the precise coordinates of the RSUs, which are known and broadcast to all vehicles.

We suppose there are two kinds of RSUs: one type positioned at road entry \\Points and the other located in the middle sections of the road between entry points. Entry RSUs broadcast the travel direction as either N or S, while middle RSUs do not specify a direction in their beacons. Upon entering the road, a vehicle establishes its travel direction according to the direction indicated by the first beacon received from an entry RSU. As the vehicle continues, it will encounter a middle RSU, which broadcasts its ID and location. The vehicle's driving direction is then updated by comparing the ID of the new RSU with the ID of the previous RSU stored in the On-Board Unit (OBU), which is initially set to null. This comparison allows the vehicle to detect any changes in direction, such as a U-turn using the road's shoulder, by recognizing a shift in RSU IDs.

Algorithm 1 describes the proposed method, assuming that RSU IDs increase in the northward direction.

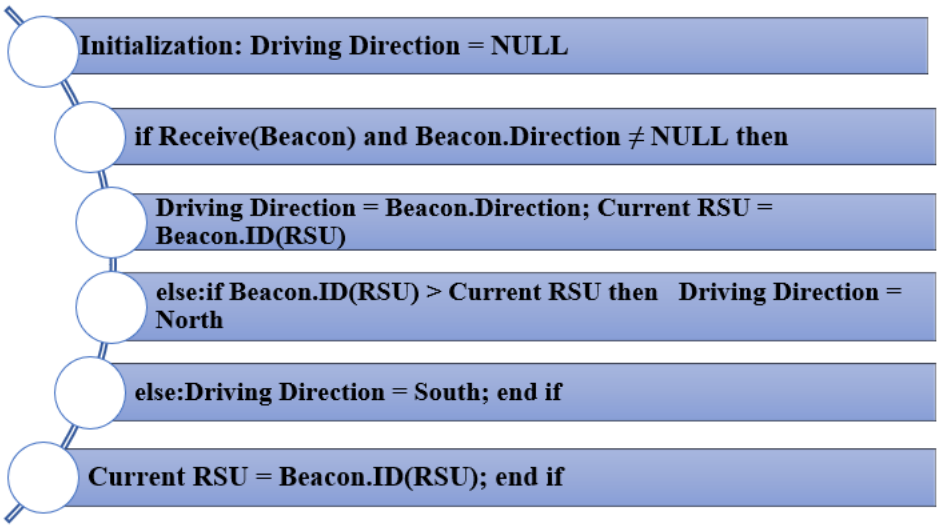


It's important to note that Algorithm 1 can be seamlessly extended to handle vehicle localization at road intersections. In these scenarios, intersection points should be equipped with Roadside Units (RSUs) that broadcast signals for all four possible travel directions: the traditional north (N) and south (S) directions, as well as the perpendicular east (E) and west (W) directions. These RSUs at the intersections serve as entry and exit points for the crossing roads. When a vehicle receives a signal from an intersection RSU, it determines if its current travel direction remains unchanged or if it has shifted to one of the perpendicular directions.

### 3.1.3. Localization System using RSU

In the analyzed method, the vehicle frequently measures its distance to the RSU using a time-of-flight (ToF) approach. From a single measurement session, only the distance $r$ can be determined; the azimuth and the RSU's exact position remain unknown. This results in a circle of radius $r$ with the RSU located somewhere along its circumference, and the vehicle positioned at the circle's center. Theoretically, the RSU's location relative to the vehicle can be determined through trilateration by conducting two measurement sessions at different vehicle positions. However, in practice, various adverse factors can distort the measurements. These include delays from communication devices, noise due to sensor imperfections on the vehicle, the

unknown height at which the RSU is mounted above the road, and more. Such factors introduce errors into the measurements, which may be systematic or random, depending on their origin.

In the proposed system, two Road-Side Units (RSUs) positioned on opposite sides of the road communicate their location details to vehicles passing through their coverage zones. Vehicles use ranging techniques like Time of Arrival (TOA) or Time Difference of Arrival (TDOA) to calculate their distance from each RSU. Utilizing the received position and distance data, vehicles draw two intersecting circles and identify their current location at the circle's intersection points. Since vehicles are aware of their travel direction, they can select the correct intersection point as their position after receiving the second RSU broadcast.

To minimize the number of required RSUs, some theories suggest a localization system that relies on only one RSU. This system employs a two-way TOA packet exchange method to facilitate control information sharing between the vehicle and the RSU, allowing distance measurement between them. This ranging technique provides only the vehicle's y-coordinate, while the x-coordinate is updated using a motion model derived from an Inertial Navigation System (INS), provided that the initial x-location is known.

In RIALS, each vehicle determines its distance to the RSU using TOA and gathers kinetic data from the INS between beacon broadcasts. This data helps form several intersecting circles, centered on the vehicle's kinetic information and the initial RSU position. The vehicle's current position is found at the intersection of these circles, with more circles improving localization accuracy.

Similar to other RSU-based approaches, the RSU periodically sends out its position information. Upon receiving this, vehicles equipped with antenna arrays estimate their position using AOA and a weighted least squares algorithm. The authors also integrate this AOA-based method into cooperative positioning systems, considering both Vehicle-to-Vehicle (V2V) and V2R communications to reduce the need for multiple location-aware neighbors and the V2V communication load.

In electronic toll collection (ETC), vehicles are tagged and detected by an RSU with a reader antenna array, which identifies the vehicle's lane and processes toll

payments simultaneously. In parking lot scenarios, the RSU estimates the vehicle's direction based on signals transmitted by the vehicle and updates as the owner moves. These systems typically focus on determining the lane or direction rather than pinpointing the vehicle's exact location.

In contrast to previous work, the current study employs RSUs with directional antennas to aid vehicles in determining their precise location.

The present work proposes a positioning structure designed for vehicles traversing specific road sections, leveraging Roadside Units (RSUs) equipped with directional antennas. The system construction for this suggested method is depicted in Figure 3.4. It is worth noting that, while assuming the organization of two RSUs on a similar side of the road, our structure can readily accommodate scenarios where they are situated on opposite sides.

Our analysis employs a directional antenna model, wherein the antenna pattern is approximated as a conical segment with an apex angle denoted as θ, in case of: $\theta \in [0, \frac{\pi}{2}]$ . As shown in Figure 3.4, the alignments of the maneuvering antennas of the two RSUs are corrected, and the gap between them is designated as dr. Every vehicle moving on the street is presumed to be busy with an On-Board Unit (OBU) product, tasked with receiving beacon messages disseminated by the RSUs. Additionally, the vehicle is equipped with a digital compass to ascertain its present way of moving and an odometer to gauge its moving distance. The messages of the beacon transmitted by the RSUs encompass the absolute coordinates of the RSU and the alignment of the RSU's directional antenna. Upon receiving two messages of beacon one from every RSU, every vehicle calculates its present location utilizing the methodology elucidated in the subsequent segment. [27]

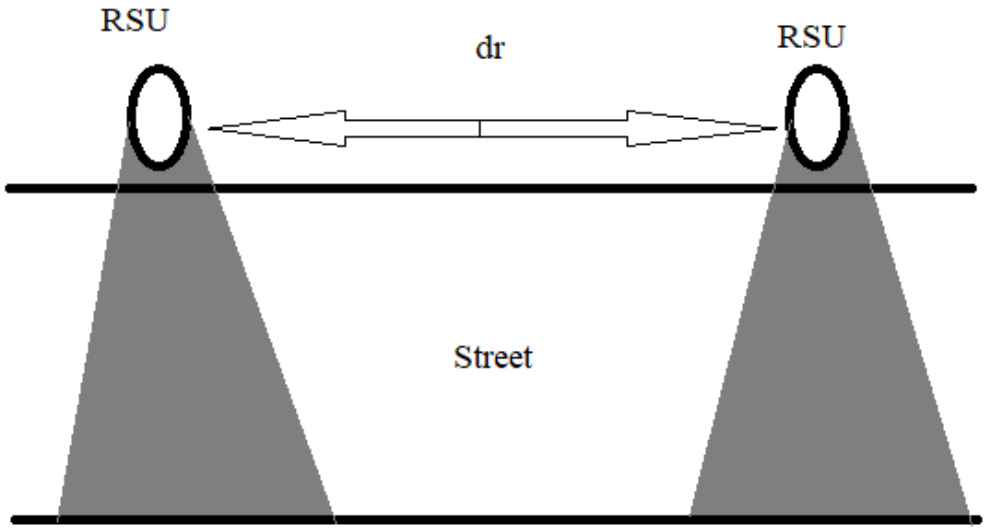


Figure 3.4. System architecture [27].

### 3.1.4. Localization Scheme for Vehicles

Let's consider a scenario where two Roadside Units (RSUs), $R_a$ and $R_b$, are positioned on the same side of the road at the same location. Additionally, let's suppose that the directional antennas of $R_a$ and $R_b$ are oriented at angles $\delta a_a$ and $\delta b_b$, correspondingly, relative to the direction of east. It's important to note that the angles are constrained within the range $0 < |\delta a_a|, |\delta b_b| < 90$ degrees. As a vehicle, denoted as V, travels lengthways along the road in a direction of north, it receives the initial message of a beacon broadcast by $R_a$ upon entering the coverage zone of its directional antenna. Upon getting the initial beacon message, which is described last, the vehicle archives the absolute location coordinates ($x_{abs}$, $y_{abs}$) of $R_a$ and the alignment angle ($\delta a_a$) of $R_a$'s directional antenna. Subsequently, as the vehicle progresses along the road, it goes into the attention zone of $R_b$'s directional antenna and then receives the corresponding initial beacon message. At this point, the vehicle incorporates the absolute location of $R_b$ ($x_b$, $y_b$) and the alignment angle ($\delta b_b$) of $R_b$'s directional antenna into the position and alignment data now saved in its memory.

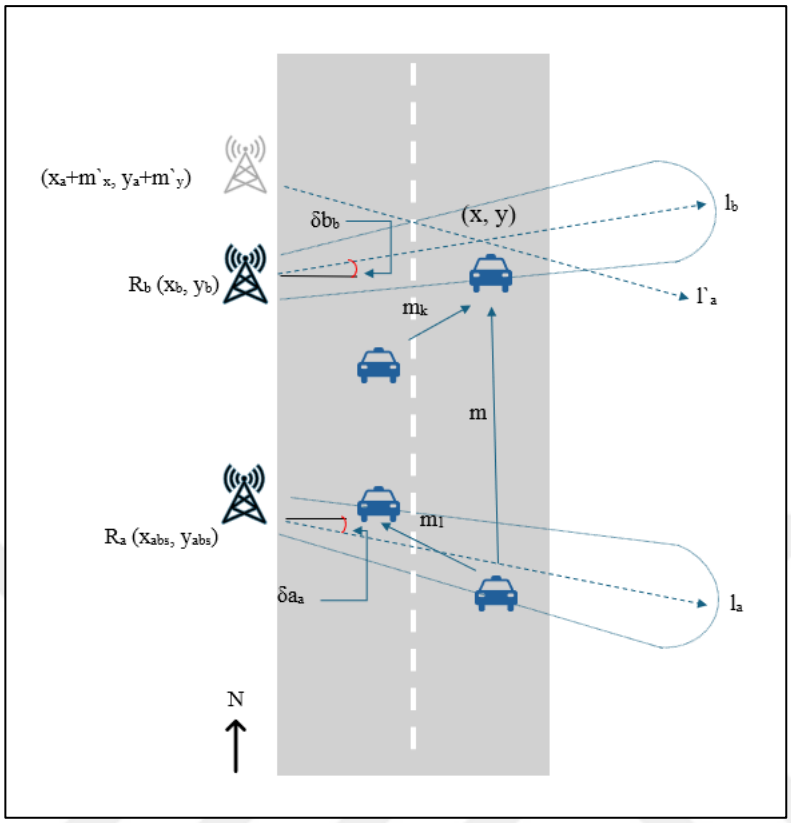


Figure 3.5. Vehicle localization scheme.

Utilizing the alignment and location data from the two beacon messages, the vehicle can compute two straight-line equations, denoted as $l_a$ and $l_b$. However, as observed in Figure 3.5, the intersection of lines $l_a$ and $l_b$ does not coincide with the actual road. Therefore, to accurately determine the vehicle's current coordinates, denoted as (x,y), the line $l_a$ needs to be adjusted based on the vehicle's displacement between the reception of the two beacon broadcasts. In real-world scenarios, vehicles often do not move in a perfectly straight line parallel to the road; they may engage in lane changes or passing maneuvers. Thus, during the positioning process, the vehicle V leverages both its odometer and digital compass to measure the total movement vectors generated by its path and the distance covered between receiving the initial beacon from $R_a$ and the one from $R_b$. To accurately adjust the line $l_a$ and estimate its current position, V must calculate the overall movement resulting from all individual movement vectors generated during this interval. Consider the example illustrated in

Figure 3.5. Assuming V executes k displacement through the interval between the two broadcasts of beacon, it produces k movement vectors, denoted as mj for j = 1, ..., k.

The combined displacement, representing the lowest distance from V's initial to destination location through the interval among the two beacon broadcasts, could therefore be calculated as:

$$m = [m_x \quad m_y] = \sum_{j=1}^{k} m_j = [\sum_{j=1}^{k} m_{j,x}, \sum_{j=1}^{k} m_{j,y}] \tag{3.1}$$

In this case, $[m_x, m_y]$ represents the vector 'm' with its x component denoted as '$m_x$' and y component as '$m_y$'.

The directional antennas' radio patterns are not limited to a direct line but instead exhibit a conical-like segment. Consequently, the point at which V receives the beacon message from $R_a$ does not precisely align with line '$l_a$'. In practical scenarios, V cannot simply choose the position where it initially receives the message of beacon from $R_a$ as the beginning point for its initial movement vector 'm1' because line '$l_a$' cannot be accurately translated. Therefore, a scheme for selecting the beginning location of the first movement vector 'm1' is proposed to ensure correct calculation of the movement vectors.

Upon receiving from $R_a$ a beacon message, V utilizes data from its odometer and digital compass to get its present location '$P_l$' relative to '$P_0$' in a position list for $R_a$, denoted as '$LocR_a = \{P_l | l = 1, ..., N\}$', where 'N' represents the value of received messages of beacon from $R_a$. Subsequently, V initiates a timer and pauses for additional beacon messages. In case there is no message received beforehand the timer elapses, the suggested chosen structure is employed to estimate the coordinates at which V interconnects line '$l_a$', denoted as '$P_s(x_s, y_s)$'. The index 's' of $LocR_a$ could be determined as:

$$s = N * [\frac{\overline{IP_0}}{P_N P_0}] = N * [\frac{\sin(\alpha + \theta)}{2\cos(\theta / 2)\sin\beta}] \tag{3.2}$$

Where:

$$\arg\alpha = \pi - a_1 - \delta - \theta/2$$

$$\arg\beta = \pi - a_1 - \delta - \theta/2$$

$$a_1 = \tan^{-1}(m_{1,y} / m_{1,x})$$

$a_1$ represents vehicle direction in the beginning vector movement.

Depending on the beginning point selection process delineated earlier, the displacement of the moving vector could be estimated as follows:

$$m' = [m'_x, m'_y] = m' + \sum_{j=2}^{k} m_j \qquad 3.3$$

In case of: $m'_1 = P_s - P_E = (x_E - x_s, y_E - y_s)$;

$P_E$ the reached location of vehicle in the first vector.

As shown in Figure 3.5. The two direct lines of vehicle relation are given as follows:

$$y - y_a - m'_y = (x - x_a - m'_x)\tan\delta_a \qquad 3.4$$

$$y - y_b = (x - x_b)\tan\delta_b \qquad 3.5$$

So, the final vehicle coordinates are given as:

$$x = \frac{y_a - y_b - x_a\tan\delta_a + x_b\tan\delta_b - m'_x\tan\delta_a + m'_y}{\tan\delta_b - \tan\delta_a} \qquad 3.6$$

$$y = y_b - x_b\tan\delta_b + x\tan\delta_b \qquad 3.7$$

In real settings, many roads accommodate traffic flow in two opposite ways. Due to limitations in space, the preceding discussions focused on the directforward scenario where the road carries traffic in only a single direction. Nonetheless, extending the suggested positioning structure to accommodate two reverse traffic flows could be readily achieved. [27]

### 3.1.5. Determining the Optimal Antenna Alignment Angle and Beam Width

In real-world settings, the transmission shape of directional antennas resembles a narrow cone rather than a good direct line. Let's consider that the beam width of each RSU is denoted as θ, and the directional antennas of corresponding RSUs within every set share a similar alignment.

For easiness, let's also consider that vehicle V, utilizing the suggested starting location chosen mechanism, can approximate its coordinate intersection with line '$l_a$' at a distance 'w' from the left sideways of the road. Furthermore, let's assume that V moves in a direct line along the road.

Upon advancing, V notices the message of beacon broadcasted by RSU $R_b$ at point C. Upon receiving this message, V employs the coordinates of RSUs $R_b$ and $R_a$, along with their respective directional antenna alignment angles (-δ and δ), to compute the joint point D between the two direct lines '$l_a$' and '$l_b$' as its expected location. Nevertheless, V is actually positioned at point C sooner than point D. In essence, a localization error, CD, is present. By applying main trigonometric bases, the magnitude of AC could be calculated as:

$$\frac{\overline{AC}}{1} = \frac{\overline{AB}}{\cos(\delta - \frac{\theta}{2})} \tag{3.8}$$

$$\overline{AC} = \frac{\omega}{\cos(\delta - \frac{\theta}{2})} = \omega \sec(\frac{\theta}{2} - \delta) \tag{3.9}$$

The magnitude of $\overline{CD}$

$$\frac{\overline{CD}}{\sin\frac{\theta}{2}} = \frac{\overline{AC}}{\sin(\pi - 2\delta)} = \frac{\overline{AC}}{\sin(2\delta)} \tag{3.10}$$

$$\overline{CD} = \omega \sec(\frac{\theta}{2} - \delta)\sin(\frac{\theta}{2})\cos(2\delta) \quad 3.11$$

To reduce the position error, CD, an optimum solution of the problem of defining the optimum antenna alignment angle and beam width could be formulated as follows:

$$(P0)\min_{\delta,\theta} f(\delta,\theta) = \omega \sec(\frac{\theta}{2} - \delta)\sin\frac{\theta}{2}\cos(2\delta) \quad 3.12$$

$$In\_case: \frac{\pi}{18} \le \theta < \pi/2; 0 < \delta + \theta/2 < \pi/2 \quad 3.13$$

The advantage of the optimization question error is to reduce the error of geometric induced by the antenna alignment beam width and angle, as depicted in Equation (3.12). Equation (3.12) specifies the limits on the beam width imposed by the road structure. Equation (3.13) ensures that the coverage of the directional antenna does not extend beyond the surface of the road.

It's worth noting that several producers have developed directional antennas with a minimum horizontal beam width of approximately 10 degrees (which means π/18). Therefore, the minimum rate of θ is set to π/18.

It is noted that 'f' is a monotonically growing function with respect to the antenna alignment angle δ, in case 0 < δ < 90 degrees. This observation holds because of

$$\frac{\partial f}{\partial \theta} = (2\sin\delta\cos(\frac{\theta}{2} - \delta)^2)^{-1} \quad 3.14$$

Given that $\theta \in \left[\frac{\pi}{18}, \frac{\pi}{2}\right]$, we could deduce that the value of 'f' could be decreased by substituting θ with its smallest value.

With this substitution, Question P1 is changed into the next question:

$$(P1)\min_{\delta} f(\delta) = \omega^* \sec(\frac{\theta}{2} - \delta)\sin\frac{\theta}{2}\cos(2\delta) \quad 3.15$$

$$In\_case: 0 < \delta < \pi / 2 - \theta \quad (3.16)$$

Equation (3.16) is derived from Equation (3.13). Problem P1 is recognized as a convex optimization problem because the impartial purpose is convex concerning δ, in case the term is linear. Consequently, Problem P1 could be effectively tackled using Newton's law. [28],

## 3.1.6. RSU Deployment

This section presents a review and categorization of various RSU deployment strategies in Vehicular Networking. Based on vehicle mobility and RSU placement strategies within geographic areas, the reviewed studies are classified into two main categories: static and dynamic deployment schemes.

Each RSU's coverage area is regarded as a logical coverage area, defined by geometric properties and dynamically expanding within a two-dimensional space. Patil and Gokhale [29] introduced a Voronoi diagram-based algorithm for efficient RSU deployment, considering packet loss and delay as key factors. The delay threshold of packets broadcast between RSUs helps define the boundaries of each polygon in the diagram; delays that exceed this threshold negatively impact service availability. Figure 3.6 illustrates the Voronoi diagram process, showing how a set of points divides the geographical area into convex polygonal cells.

The resulting RSU map often reveals significant overlapping areas between RSUs. To address these overlaps and any missed areas, the farthest reaches of each two neighboring RSUs are considered. Elements including traffic density and intersection significance have minimal impact on this approach. However, the deployment sites identified by this method are not always suitable for RSU installation due to potential issues like private property boundaries, natural obstacles such as rivers, and the presence of buildings.

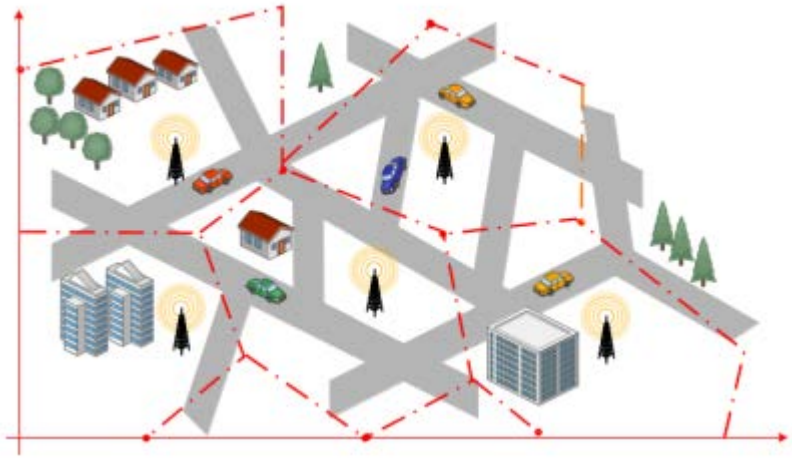

Figure 3.6. Voronoi diagram methodology for putting of RSU in an urban area.

Ghorai and Banerjee [30] developed a Constrained Delaunay Triangulation (CDT) strategy to enhance RSU deployment optimization. This approach divides the topological area into multiple convex triangles, where the vertices represent potential RSU locations, ensuring that no RSUs are positioned within the circle around every triangle (see Figure 3.7).

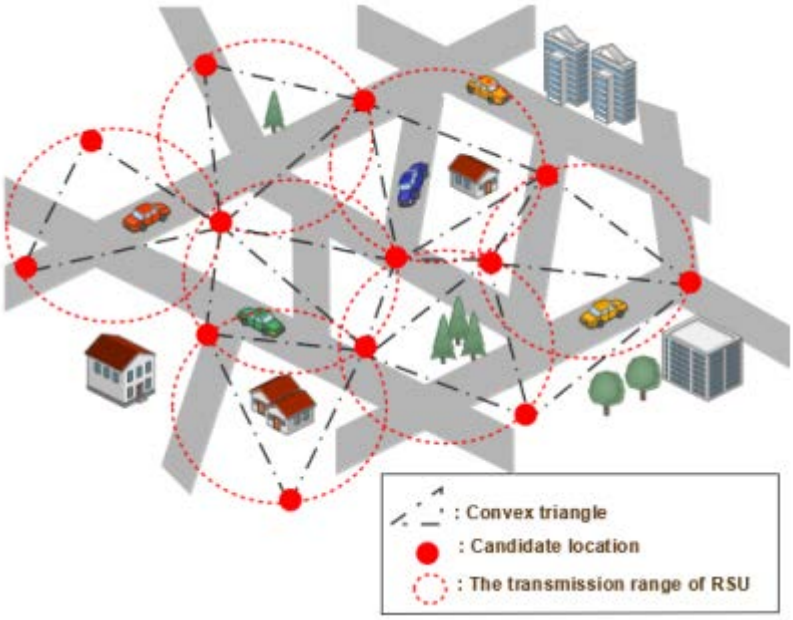


Figure 3.7. Constrained Delaunay triangulation approach.

Clearly, maintaining an accurate and up-to-date estimation of the vehicle's location along the road requires more than just two RSUs. However, installing supplementary RSUs necessitates a careful balance between achieving high localization accuracy and minimizing deployment costs. To address this trade-off, the current study recommends effective installation of Roadside Units (RSUs). designed to meet both objectives.

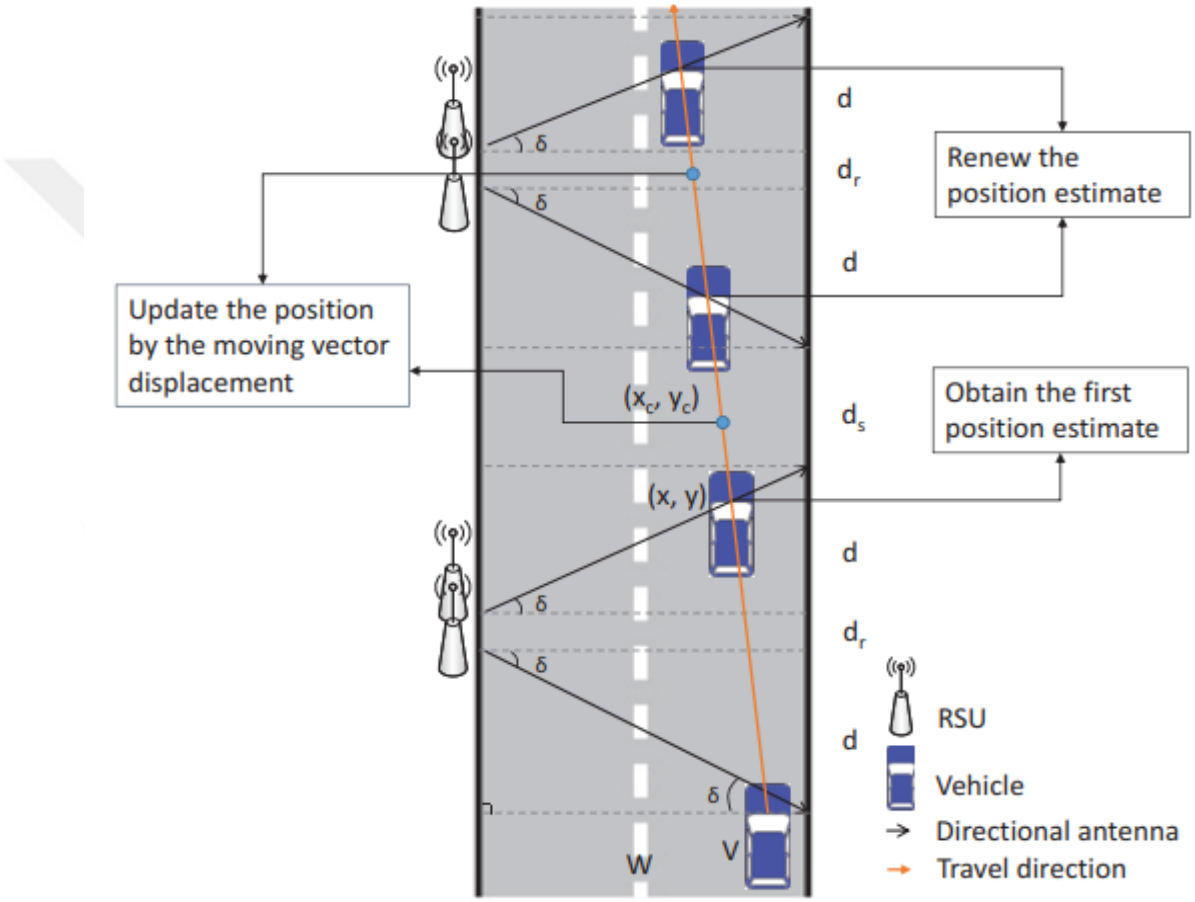


Figure 3.8. RSU deployment. [27]

Let's denote W as the width of the road, then δ is the alignment angle of the RSU directional antennas. Figure 3.8 outlines the suggested RSU deployment technique, where the beginning RSU is positioned at a distance d from the beginning of the road, ensuring that all vehicles entering the road unavoidably pass over its coverage zone. Employing main trigonometric relations, the value of d could be calculated as:

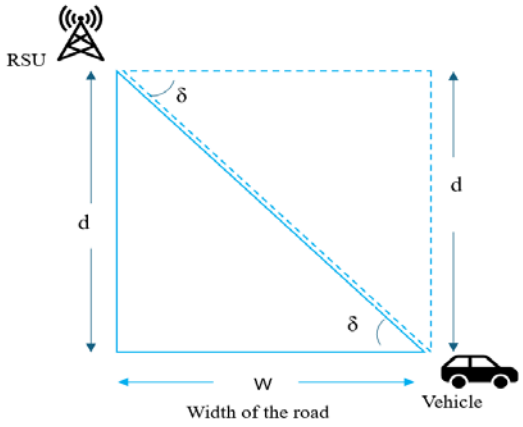


$$\frac{W}{\cos\delta} = \frac{d}{\sin\delta} \tag{3.17}$$

$$d = \frac{W\sin\delta}{\sin(\frac{\pi}{2} - \delta)} \tag{3.18}$$

After determining the location of the first RSU, the distance between nearest RSUs within a set is designated as dr. Additionally, the gap among the nearest RSU groups is defined as ds. It's important to notice that the value of ds directly influences the RSU deployment cost. A lesser value of ds leads to an increased whole number of RSUs needed to uphold accurateness along a road of an agreed distance, and vice versa. It's crucial to highlight that the optimum RSU deployment strategy involves setting ds = 0 to achieve the highest positioning accuracy [31], [32].

As depicted in Figure 3.8, once the RSUs are deployed, a vehicle V incoming the road establishes its initial location estimate (x, y) upon messages of beacon are receiving from the beginning two RSUs. Subsequently, the vehicle begins measuring its displacement vector $m_c = [m_{c,x}, m_{c,y}]$ and updates its present coordinates $(x_c, y_c)$ accordingly.

$$(x_c, y_c) = m_c(x, y) = (m_{c,x}x, m_{c,y}y) \tag{3.19}$$

Upon receiving the message of beacon from the subsequent RSU, V updates its position estimate using previous equations from the proposed localization scheme. This iterative process allows the vehicle to continuously estimate its location as it progresses through the road, effectively integrating the RSU deployment approach with the suggested localization approach.

## 3.1.7. Tolerance Toward RSU Errors

In real scenarios, RSUs might encounter malfunctions or complete failures due to various factors such as crashes, inadequate maintenance, or severe weather conditions. Such RSU errors unavoidably disrupt the usual operation of the suggested positioning structure. Therefore, this segment introduces a location update technique for vehicles encountering impermanent RSU failures.

Assuming the scenario depicted in Figure 3.9, where $R_{a2}$ experiences a failure, leaving only $R_{b2}$ operational. In this situation, vehicle V estimates its present coordinates (x1, y1) depending on the beacon messages received from $R_{a1}$ and $R_{b1}$. After updating their position coordinates using the messages of the beacon from two RSUs, vehicles continuously update their locations utilizing equation (3.19) until they receive the next beacon message.

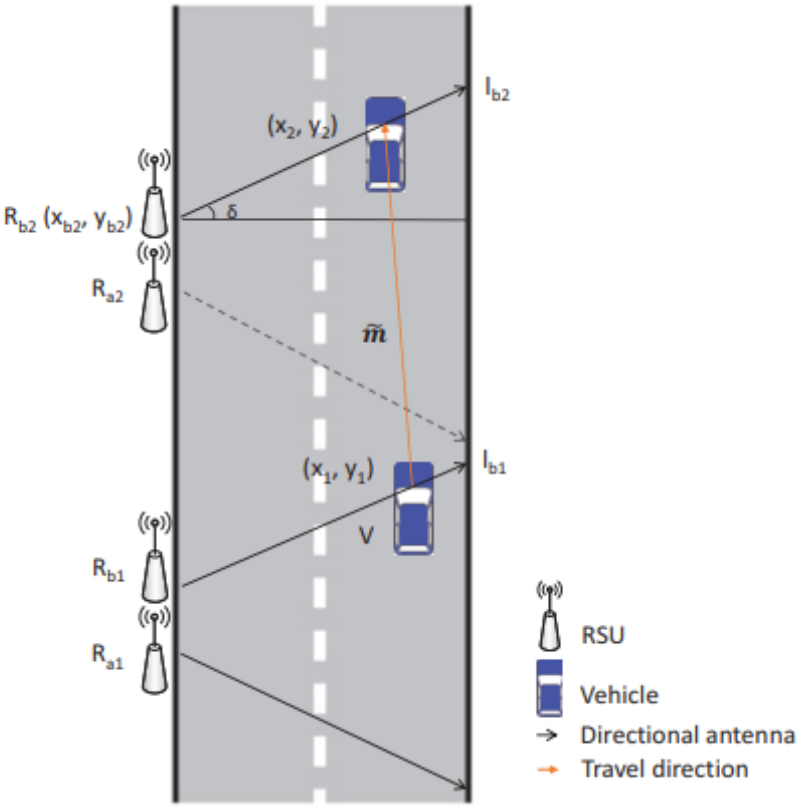


Figure 3.9. Position update using single RSU.

Thus, vehicle V could still update its location during traveling between the radio patterns of $R_{b1}$ and $R_{b2}$ despite the failure of $R_{a2}$. However, upon receiving the message

of the beacon from $R_{b2}$, the localization method described in equations (3.19) and (3.20) cannot be executed accurately since the antenna alignments of $R_{b1}$ and $R_{b2}$ are identical. Consequently, the location coordinates could not be determined utilizing the suggested intersection-point structure because that: for two lines which are parallel, no such point occurs.

Therefore, vehicle V estimates its novel location, (x2, y2), depending on its displacement vector m˜ =[˜mx, m˜ y] and the message of beacon received from $R_{b2}$.

The novel location of V, (x2, y2), is calculated by resolving the joint of the two direct lines $l_{b2}$ and m˜, expressed correspondingly as

$$y - y_{b2} = (x - x_{b2}) \tan \delta \qquad 3.20$$

$$y - y_1 = (x - x_1) \frac{m_y}{m_x}$$

## 3.2. METHODOLOGY

In this study, we investigate a vehicular network consisting of a four-lane traffic system that facilitates two-way movement. This network incorporates two types of connected devices: onboard units (OBUs) installed within vehicles and Roadside Units (RSUs) positioned along the road. Vehicle localization within this network relies on Received Signal Strength (RSS) information, which is derived from the Received Signal Strength Indicator (RSSI) that can be easily extracted from a regulated message set. The RSSI measures the signal strength transmitted by the RSU, and this information is temporarily stored within the OBU device before potentially being uploaded to cloud servers.

For simplicity, we assume that the vehicles' positions can be represented using a two-dimensional (2D) coordinate system. In this system, the X and Y axes are

assumed to be perpendicular and parallel to the lanes, respectively. The unknown coordinates of a vehicle with index j are denoted as

$$\theta_j = [a_{j,1}, a_{j,2}]^T : \theta_j \in \mathrm{R}^2, where j = 1, ...., M \quad 3.21$$

and the RSU with indexed i coordinates are written as:

$$\Phi_i = [b_{i,1}, b_{i,2}]^1 : \Phi_i \in \mathrm{R}^2, i = 1, ...., N \quad 3.22$$

In this context, M represents the entire number of vehicles, while N denotes the maximum number of RSUs with which each vehicle can establish communication. This capability is determined by various factors such as the communication range and transmission power of the RSUs. The origin of the coordinate system for each deployment is labeled as O and is depicted in the corresponding plot at coordinates (0,0).

## 3.2.1. Waveform Propagation Model

Accurate localization relies heavily on the modeling of waveform propagation. Various wireless communication channel models are available, including the Okumura-Hata model, the Lee model, typical indoor models, attenuation factor models, direct loss models, and logarithmic path loss model. Among these, the logarithmic path loss model suggests that the path loss of waveform propagation is logarithmically related to the increase in distance. This model can be considered a straightforward and practical representation of waveform propagation characteristics in traffic scenarios. The power of received waveform at the vehicle with index j transmitted from the ith RSU, meant as $P_{i,j}$, is linked to their distance utilizing the model of logarithmic path loss.

$$P_{i,j} = P_0 + m_{i,j} + 10 * \gamma * \log_{10} \frac{\left\| \theta_j - \Phi_i \right\|}{d_0} \quad 3.23$$

where $P_0$ represents the power of the received waveform at a distance d0 which is considered as a reference distance ($\left\|\phi_i - \theta_j\right\| \geq d_0$).

$\left\|\phi_i - \theta_j\right\|$ represents the Euclidean distance between the ith RSU and the jth vehicle, and "mi,j" represents the noise.

Typically, "mi,j" is formed as a zero-mean random Gaussian variable with a normal difference symbolizing shadowing, that could be written as: $m_{i,j} : N(0, \sigma_{i,j}^2)$

The path-loss exponent (PLE), represented by γ and usually falling within the range of 2 to 6, is regarded as an ecological factor prejudiced by the nearby conditions. Utilizing the measurements of RSS and environmental factors, we approximate the parametric positioning issue for the jth vehicle using Eq. (3.23) to determine its position θ [33].

## 3.2.2. Problem Statement

Depending on the position of the jth vehicle, the nonlinear model is:

$$f(\theta_j - \Phi_i) = P_0 + 10\gamma \log_{10} \frac{\left\|\theta_j - \Phi_i\right\|}{d_0} \qquad 3.24$$

In case we expect that estimation, blunders are autonomous and indistinguishably dispersed, the Most extreme Probability (ML) estimator for the RSS-depending positioning issue could be determined as:

$$\theta_j = \arg\min_{\theta_j} \sum_{i=1}^{N} (-(P_{i,j} - P_0) + 10\gamma \log_{10} \frac{\left\|\theta_j - \Phi_i\right\|}{d_0})^2 \qquad 3.25$$

Depending on the previously mentioned contemplations, three challenges hinder the coordinate utilization of Eq (3.24) for vehicle positioning in energetic C-V2X systems. Basically, it is famous that the initial ML estimator shows a profoundly non-convex space $\{\theta_j \mid \theta_j \neq \Phi_i\}$ is noncontinuous.

Furthermore, the C-V2X waveform is integrally more prone to packet loss in traffic situations likened to static sensor networks. Moreover, Eq. (3.25) incorporates terms $\log_{10}\left\|\theta_j - \Phi_i\right\|$ that do not render the impartial function convex or concave. While it's conceivable to restrain these terms within a convex domain $\theta_j$ (as established by inspecting the Hessian of $\log_{10}\left\|\theta_j - \Phi_i\right\|$ that is neither semi-definite positive nor semi-definite negative), this approach has been unreasonable caused by waveform variations persuaded by quickly traveling goals in traffic situations, making position and verifying a universal smallest solution stimulating. A convex estimator will be very needed; the presence of $\log_{10}\left\|\theta_j - \Phi_i\right\|$ creates like an idea worrying.

At that point, inside energetic C-V2X systems, vehicles navigate different street situations, such as urban timberlands and regions with high rises, driving to varieties within the natural components shown in relation (3.25). Moreover, wireless waveform weakening could be prejudiced by parameters such as multi-path fading, deflection, reflection, and weather situations. Considerable vehicle shadowing also affects the communication of V2V in Style C-V2X networks, as discovered by Nguyen et al. Thus, inaccurate valuation of environmental factors could render the localization system vulnerable.

Finally, Equation (3.25) is determined from a system custom-fitted for inactive sensor systems, accepting that the target moves haphazardly, and its area can, as it were be computed depending on single-snapshot perceptions at each time interim. Be that as it may, in activity scenarios, there exists earlier data. For illustration, the target's position within the going before minute shows a solid spatial and transient correlation with its area within the ensuing minute. Also, longitudinal and horizontal movement characteristics could be characterized and modeled utilizing numerical representations [34].

### 3.2.3. Overview of CV2X-LOCA

The objective of the present work is to create a solid C-V2X-dependent vehicle positioning system competent in overcoming the challenges mentioned prior and accomplishing lane-level situating precision indeed within the nonappearance of GNSS signals. The proposed localization system, referred as CV2X-LOCA, is planned to address these challenges successfully. Specifically, CV2X-LOCA consists of four essential components:

- Information preparing module.
- Coarse situating module.
- Environmental factors rectification module.
- Vehicle direction sifting module.

These modules work together to handle the inborn challenges of energetic C-V2X systems. In the case of using C-V2X communications, (OBU) introduced on a vehicle intermittently transmits messages to adjacent organized hubs, counting other vehicles, framework, and people on foot to supply and overhaul data around itself. For occurrence, the vehicle can broadcast sensor information such as GNSS positions by means of Class Awareness Message (CAM), characterized by ETSI and commonly utilized in Europe, or Basic Security Message (BSM), characterized by SAE and ordinarily utilized within the U.S. Additionally, Roadside Units (RSUs) could be considered communicable foundations with profoundly precise location data, but obscure transmit control. We recognize the potential for tumult obstructions through C-V2X waveform transmission, and waveform parcels may vary or end up misplaced due to the high versatility of vehicles and other natural objects.

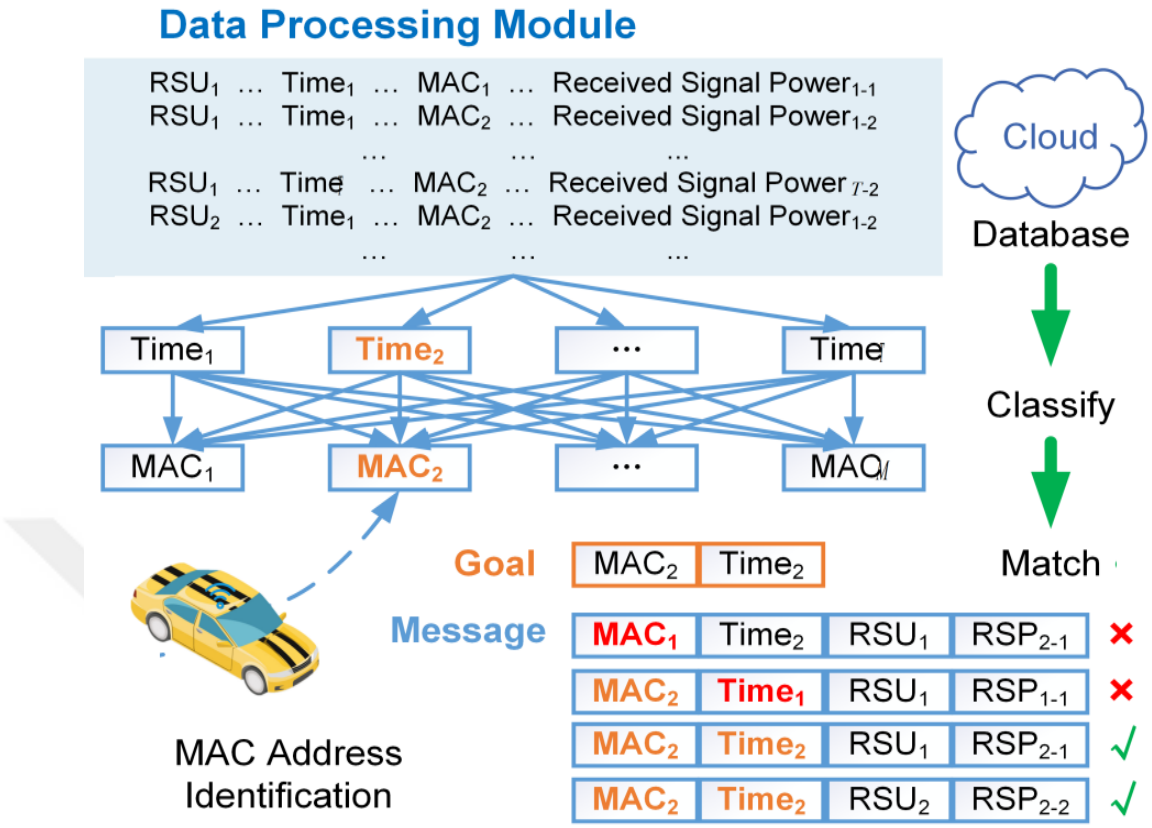


Figure 3.10. 3-B Data processing module.

We recommend an information handling module, portrayed in Figure 3.10, to synchronize information from several OBUs. The lattice Gi speaks to the waveform dataset gathered by total vehicles from the ith RSU amid the discovery time T, which saved in climbing time arrange. The information tests are organized as follows:

Gi={00:16:EA:AE:3C:30, 7/10/2021 10:20:30, -68;}, where "00:16:EA:AE:3C:30" indicates the one-of-a-kind Media Get to Control (MAC) address for every vehicle, "7/10/2021 10:20:30" speaks to the timestamp, and "-68" means the gotten waveform control values among total vehicles and the ith RSU.

Essentially, we characterize the lattice Gj as the waveform dataset gathered by the jth vehicle from all RSUs amid the location time T, orchestrated in rising time arrange. The information tests are organized as follows:

Gj={7/10/2021 10:20:30, RSU1, -68;}, in case "RSU1" signifies the supreme arrange location of the primary RSU. By adjusting these datasets utilizing as identifiers

both interesting MAC addresses and timestamps, able to get test information collected by all RSUs as takes after:

$$G_{i,j} = \begin{bmatrix} MAC_j, 7/10/202110:20:30, RSU1, -68 \\ MAC_j, 7/10/202110:20:30, RSU1, -66 \end{bmatrix} \quad 3.26$$

With the data processing described, we can integrate the information collected from each vehicle by all RSUs during the detection period T. In this context, the first row represents the data gathered by the first RSU from the $j_{th}$ vehicle at time t, and so on [35], [36].

## 3.2.4. Coarse Positioning Module

Given the non-convex and nonlinear nature of the objective process in the usual ML estimator of Equation (3.25), we propose a coarse positioning module inspired by the newly developed SDP-depending framework. Our module is specifically designed for vehicle localization in dynamic C-V2X networks.

To begin, we aim to eliminate the logarithm of residuals in Eq. (3.25). We can define a residual as

$$r_{i,j} = -(P_{i,j} - P_0) + 10\gamma \log_{10} \frac{\left\| \theta_j - \Phi_i \right\|}{d_0} \quad 3.27$$

Where $r_{i,j}$ represents the dissimilarity among the real position and the value of measurement. Thus, Equation (3.25) could be interpreted as minimizing a penalty purpose on the residual vector

$r = [r_{1,j}, ...., r_{N,j}]^T : (r \in ¡^N)$

As

$$\hat{\theta}_j = \arg\min_{\theta_j} f(r) \quad 3.28$$

Where: $f(.) = \|.\|^2$

To develop an estimator of nonconvex not including the logarithm in the remainders, we swap $f(.) = \|.\|^2$ with extra function of penalty $f(.) = \|.\|_\infty = \max|[.]_i|$ that represents the norm of Chebyshev, that is recognized as the $l_\infty$.

$$\hat{\theta}_j = \arg\min_{\theta_j} \max_i \left| -(P_{i,j} - P_0) + 10\gamma \log_{10} \frac{\|\theta_j - \Phi_i\|}{d_0} \right| \quad 3.29$$

After certain manipulations, we shall be able to formulate the same problem without involving, as below:

While $\|\theta_j - \Phi_i\| > 0$ and the minimizer are not pretentious by the positive scaling of the objective function, so Equation 3.29 could be written as follows:

$$\hat{\theta}_j = \arg\min_{\theta_j} \max_i \left| \log_{10} \frac{\|\theta_j - \Phi_i\|^2}{\beta_{i,j}^2} \right| \quad 3.30$$

With attention to the next equation:

$$\left| \log_{10} \frac{\|\theta_j - \Phi_i\|^2}{\beta_{i,j}^2} \right| = \max(\log_{10} \frac{\|\theta_j - \Phi_i\|^2}{\beta_{i,j}^2}, \log_{10} \frac{\beta_{i,j}^2}{\|\theta_j - \Phi_i\|^2}) \quad 3.31$$

Using mathematics scales, the equation 3.31 could be formulated as:

$$\left| \log_{10} \frac{\|\theta_j - \Phi_i\|^2}{\beta_{i,j}^2} \right| = \log_{10} \max(\frac{\|\theta_j - \Phi_i\|^2}{\beta_{i,j}^2}, \frac{\beta_{i,j}^2}{\|\theta_j - \Phi_i\|^2}) \quad 3.32$$

So, we can write:

$$\hat{\theta}_j = \arg\min_{\theta_j} \max_i \log_{10}(\max(\frac{\beta_{i,j}^2}{\left\|\theta_j - \phi_i\right\|^2}, \frac{\left\|\theta_j - \phi_i\right\|^2}{\beta_{i,j}^2})) \quad 3.33$$

However, it's known that the logarithmic function $\log_{10}$ is strictly monotonically increasing within it range from zero to infinity. Therefore, the logarithmic function is maximized when the variable "x" is maximized. Hence, we can write:

$$\hat{\theta}_j = \arg\min_{\theta_j} \max_i \max(\frac{\left\|\theta_j - \phi_i\right\|^2}{\beta_{i,j}^2}, \frac{\beta_{i,j}^2}{\left\|\theta_j - \phi_i\right\|^2}) \quad 3.34$$

Where:

$$\beta_{i,j}^2 = d_0^2 10^{\frac{P_{i,j} - P_0}{5\gamma}} \quad 3.35$$

We offer a comprehensive derivation and confirmation of Eq. (3.35). The suggested estimator for the CV2X-depending vehicle positioning problem taken into consideration in this work could be succinctly expressed as

$$\hat{\theta}_j = \arg\min_{\theta_j} f(\text{P}\%\text{þ} \quad 3.36$$

Where

$\text{P}\%\text{o} = [\text{P}\%_{1,j}, ...., \text{P}\%_{N,j}]^T : \text{P}\%_{i,j} \in \text{¡}^N$ is the suggested residual vector, that could be expressed as

$$\text{P}\%_{i,j} = \max(\frac{\beta_{i,j}^2}{\left\|\theta_j - \phi_i\right\|^2}, \frac{\left\|\theta_j - \phi_i\right\|^2}{\beta_{i,j}^2}) \quad 3.37$$

- (The Estimator Rationality): Upon closer checking of Equation (3.37), it becomes apparent that it could be expressed as

$$\beta^2{}_{i,j} = 10^{\frac{m_{i,j}}{5}} \left\|\theta_j - \phi_i\right\|^2 \quad 3.38$$

Equation (3.36) and Equation (3.37) prove that a multiplicative model is exist in the noise in $\beta^2{}_{i,j}$ , the noise $m_{i,j}$ j is multiplicative $\left\|\theta_j - \phi_i\right\|^2$.

Eminently, it could be spoken to as an added substance demonstration. The remaining $\rho_{i,j}$ in Eq. (3.13) is additionally steady with such a multiplicative clamor show, since it contains as it were the proportion $\frac{\left\|\theta_j - \phi_i\right\|^2}{\beta_{i,j}^2}$ and its opposite.

- However, it is non-convex based on the non-convexity of the expression $\frac{\beta_{i,j}^2}{\left\|\theta_j - \phi_i\right\|^2}$. Then, this work would present the way of enhancing a convex estimator depending on the derived non-convex estimator Eq. (3.12)

## 3.2.5. Convex Estimator Establishment

Let's consider $k_i = \left\|\phi_i\right\|^2$. Depending on Chebyshev process, a nearer checking of $\left\|\theta_j - \phi_i\right\|^2$ in estimator Equation (3.36) shows that it could be expressed as

$$\left\|\theta_j - \phi_i\right\|^2 = k_i - 2\phi_i^T\theta_j + \theta_j^T\theta_j \quad 3.39$$

With defining another parameter:

$$\mu = [\mu_{1,j}, ...., \mu_{N,j}]^T : X : X \in S^2 and, \mu_{i,j} \in ¡^N \quad 3.40$$

So, the Equation (3.35) could be expressed in terms of μ and X as

$$(\hat{\theta}_j, \hat{X}, \hat{\mu}) = \arg\min_{\theta_j, X, \mu} f(\mu) \quad 3.41$$

After that:

$$tr(X) + k_i - 2\phi_i^T \theta_j \leq \mu_{i,j} \beta_{i,j}^2 \quad 3.42$$

Let us consider the auxiliary variable

$$\mu = [\mu_{1,j}, ....., \mu_{N,j}]^1 : \mu \in ¡^N \quad 3.43$$

So, equation 3.32 could be written as follows:

$$(\hat{\theta}_j, \hat{u}) = \arg\min_{\theta_j, u} f(u) \quad 3.44$$

And we have:

$$\frac{\beta_{i,j}^2}{\left\|\theta_j - \phi_i\right\|^2} \leq \mu_{i,j} \quad 3.45$$

Then the minimization problem which is represented in equation 3.45 could be presented as:

$$(\hat{\theta}_j, \hat{u}) = \arg\min_{\theta_j, u} f(u) \quad 3.46$$
$$\mu_{i,j}{}^{-1} \beta_{i,j}^2 \geq \left\|\theta_j - \phi_i\right\|^2$$

It is clear that Equation (3.45) and Equation (3.46) are equal, since the constraints in Equation (3.46) already imply that.

$$\left\|\theta_j - \phi_i\right\|^2 \neq 0; \mu_{i,j} > 0 \quad 3.47$$

So, we could write:

$$X = \theta_j \theta_j^T \quad 3.48$$

The affine term, which is represented as follows

$$tr(X) + k_i - 2\phi_i^T \theta_j \le \mu_{i,j} \beta_{i,j}^2$$

In another hand the following equation $tr(X) + k_i - 2\phi_i^T \theta_j \ge (\mu_{i,j} \beta_{i,j}^2)^{-1}$ is convex relation because of

1- tr(X) are linear in X,

2- $-2\theta_j \phi_i^T$ is linear $\theta_j$

3- $\mu_{i,j}^{-1}$ is convex in case of $\mu_{i,j} > 0$

But the equivalence term $X = \theta_j \theta_j^T$ is non affine. So, equation 3.32 is still non-convex.

To improve a convex estimator, we change the relation $X = \theta_j \theta_j^T$ to $X \ge \theta_j \theta_j^T$.

Thereby, Eq. (3.37) could be expressed as a linear matrix dissimilarity (LMI) by leveraging a Schur match. Consequently, the CV2X-depending on vehicle positioning problem could be relaxed to the next usual SDP problem

$$(\hat{\theta}_j, \hat{X}, \hat{\mu}) = \arg\min_{\theta_j, X, \mu} f(\mu) \qquad 3.50$$

$$tr(X) + k_i - 2\phi_i^T \theta_j \le \mu_{i,j} \beta_{i,j}^2$$

$$\begin{bmatrix} X & \theta_j \\ \theta_j^T & 1 \end{bmatrix} X \ge 0$$

Eq. (3.40) is convex and could be resolved utilizing an advanced technique. In this way, ready to ensure that the arrangement to the issue is additionally the worldwide least. So also, ready to express

$$tr(X) + k_i - 2\phi_i^T \theta_j \ge (\mu_{i,j} \beta_{i,j}^2)^{-1} \qquad 3.51$$

As:

$$\begin{bmatrix} tr(X) + k_i - 2\phi_i^T \theta_j & \beta_{i,j}^2 \\ \beta_{i,j}^2 & \mu_{i,j} \end{bmatrix} \ge 0 \qquad 3.52$$

A good acreage of translating Eq. (3.20) to Eq. (3.22) is that $\mu_{i,j}$ is avoided in the relation, and the restrictions become linear.

- (Relaxation Equivalence): The Eq. (3.18) is different from Eq. (3.20) with the following:

  This work relaxes the relation limitation in Eq. (3.18) to a dissimilarity limitation in Eq. (3.20). As a result, if the solution of Eq. (3.20) be suitable for $\hat{X} = \theta_j \theta_j^T$, we could assume that θj given by Eq. (3.20) is the total minimizer of Eq. (3.19), and the total minimum of Eq. (3.12) (when Eq. (3.19) is equal to Eq. (3.12)).

  $\theta_j$ which is specified by Eq. (3.20) is still feasible for Eq. (3.12), excepting $\theta_j = \phi_i$, when Eq. (3.12) is unimpeded in case $\{\theta_j \mid \theta_j \neq \phi_i\}$.

  Also, f(μˆ) which is specified by Eq. (3.20) offers a lesser bound on the optimum value of Eq. (3.12), then we solve a relaxed problem on a larger set.

## 3.2.6. Filtering of Vehicle Trajectory

Module depending on the project of [37], we have outlined a vehicle direction sifting module that coordinates earlier activity data, particularly vehicle movement highlights, to make strides in lane-level position exactness. The vehicle movement demonstrated, as classified by [37], comprises four bunches depending on longitudinal and horizontal movement highlights for customary street driving. For this ponder, we embrace the Camera VLC (CVLC) shown as the vehicle movement show. The CVLC demonstrates accept no speeding up or braking for the vehicle movement. The vehicle state space of the CVLC show could be characterized like in [37].

$$\dot{\theta} = [x \quad v_x \quad y \quad v_y] \tag{3.53}$$

where x represents lateral location, y represents longitudinal location, $v_x$ and $v_y$ depending on the lateral velocity and longitudinal velocity of the vehicle in the moving

location. Moreover, $\dot{\theta}$ represents the perfect situation of the vehicle. The change of state represented as:

$$\dot{\theta}(\Delta t + t) = \dot{\theta}(t) + \Delta f(t) \tag{3.54}$$

Where $\Delta t$ exemplifies the frequency of discovery, and Δf(t) in the change of situation which determined as

$$\Delta f(t) = \begin{bmatrix} 1 & 0 & \Delta t & 0 \\ 0 & 1 & 0 & \Delta t \\ 0 & 0 & 1 & 0 \\ 0 & 0 & 0 & 1 \end{bmatrix} \tag{3.55}$$

## 4.2.7. Filter Considering Uncertainty

In this context, it is essential to consider the uncertainty arising from the noise measurement and processing noise when predicting vehicle trajectories. We recognize that the vehicle trajectory filtering problem is nonlinear and can be described as follows:

$$\dot{\theta}(\Delta t + t) = Q(t) + \Delta f(\dot{\theta}(t), t) \tag{3.56}$$

And

$$\dot{z}(t) = R(t) + h(\dot{z}(t), t) \tag{3.57}$$

where f is the movement work, Q is the framework clamor (characterized as the Gaussian clamor), $\dot{z}(t)$ is the perception components, h is the perception work, and R is the perception confusion. A few procedures have been proposed to address vulnerability, such as UKF, KF, and EKF. Jondhale et al. [38] illustrated that the following execution of UKF is superior to KF/EKF in remote detecting systems. In this work, the UKF is used to handle instability within the vehicle direction channel. The connection among the vehicle's estimated area obtained from Eq. (3.40) and its area after UKF could be communicated as

$$[\hat{x}, \hat{y}]^T = g_{ukf}(\hat{\theta}) \quad 3.58$$

Where $g_{ukf}$ represents to the function UKF. The out of the UKF process, represented as $[\hat{x}, \hat{y}]^T$ is represents the destination vehicle's location coordinate.

While the theoretical foundation of CV2X-LOCA is based on Semi-Definite Programming (SDP) concepts discussed in this chapter, to ease implementation and verification, we have used the Least Square Estimation (LSE) method in the simulations (next chapter). This has been done to reduce computational complexity without sacrificing acceptable accuracy levels for the proposed application significantly.

# CHAPTER 4. SIMULATION and RESULTS

## 4.1. SYSTEM MODELLING

For simulate the algorithm in Matlab, at the beginning a function of calculation LSE is coded in Matlab, Figure 4.1 shows the flowchart of the code:

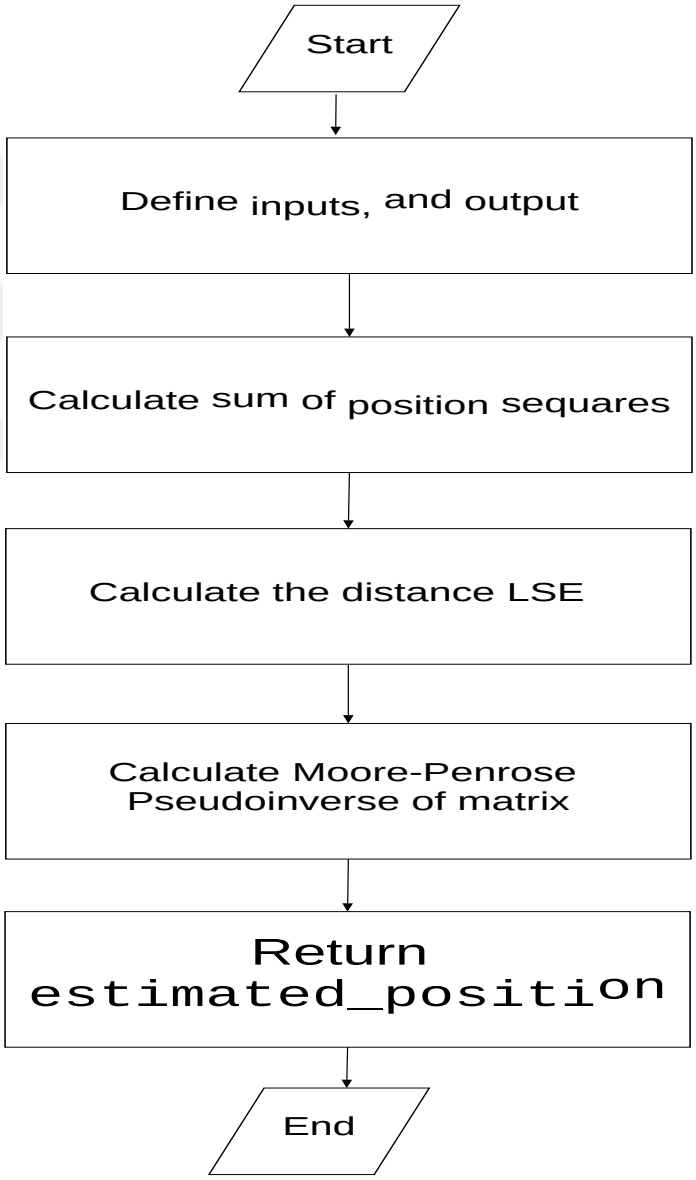


Figure 4.1. LSE procedure flowchart.

Figure 4.2 illustrates the flowchart of code programming in MATLAB for initiating Kalman filter factors and updating these factors.

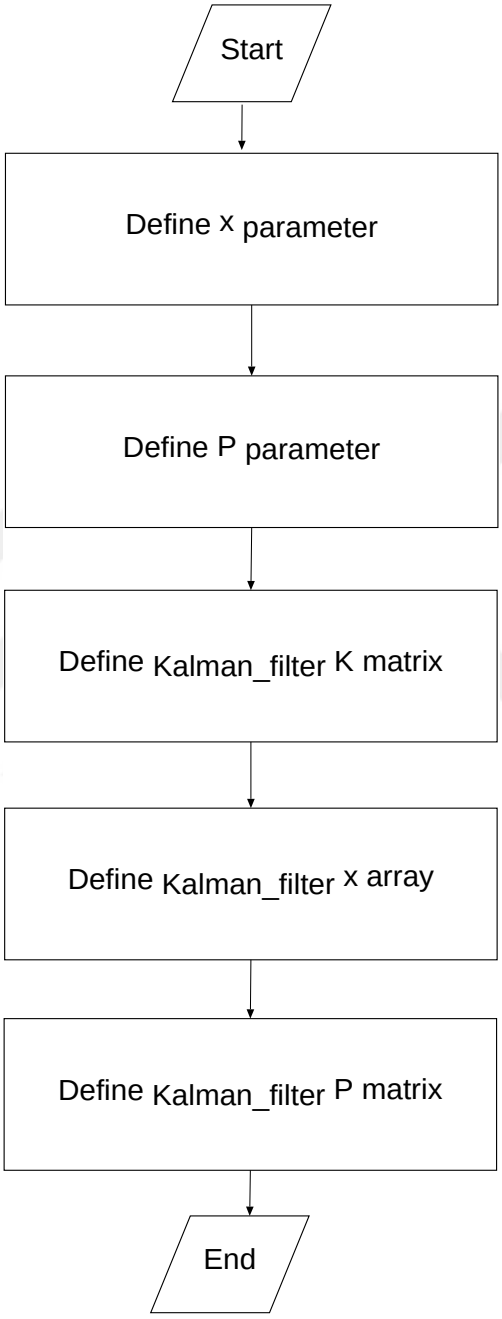


Figure 4.2. Flowchart of Kalman filter process.

Figure 4.3 illustrates the flowchart of location error defining utilizing KF.

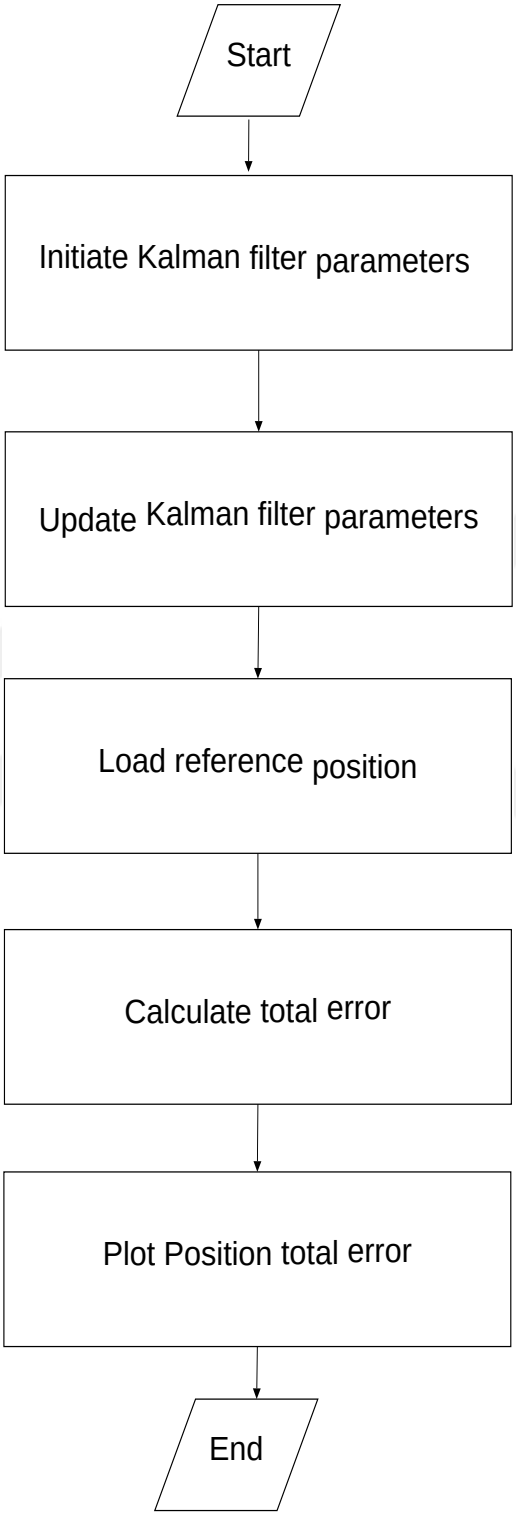


Figure 4.3. Flowchart of location error defining utilizing KF in MATLAB.

## 4.2. SIMULATION RESULT

For simulation we choose scenario from real life, so the parameter of simulation is shown in the next table:

Table 4.1: Simulation factors

| Factors | Symbol | Value |
|---|---|---|
| Ref. distance | $d_0$ | 100cm |
| Vehicle velocity | $v_x$ | 25000m/h |
| RSUs numbers | N | 3 |
| Deviation of Shadowing typical | $\sigma_{dB}^2$ | 2dBm |
| Frequency of detection | Δt | 100ms |
| Spacing of deployment | $dr_1$ | 60000cm |
| Distance | dr2 | 100cm |
| Road width | dr3 | 1400cm |
| Anchor nodes | | 4 |

Localization errors might stem from imprecisions in movement vector estimations. To guarantee steady assessment of strategy execution, we embraced, Root Mean Square Error (RMSE), Mean Absolute Error (MAE), and Mean Absolute Percentage Error (MAPE) as assessment measurements. Our evaluation criteria differ from those used by [39], [40], who focus solely on longitudinal errors perpendicular to the road. Instead, we consider 2D coordinate errors that encompass both longitudinal and lateral errors, offering a more realistic approach for real-world traffic scenarios. We performed 100 simulation runs for each scenario, fine-tuning the parameters of each method to achieve optimal performance. This included adjusting the noise covariance matrix $Q$, the measurement noise covariance matrix $R$, and the initial covariance matrix $Z0$ used in the Kalman Filter (KF).

$$R = \begin{bmatrix} 2.2 & 0 & 0 & 0 \\ 0 & 1.2 & 0 & 0 \\ 0 & 0 & 0.9 & 0 \\ 0 & 0 & 0 & 0.5 \end{bmatrix} \tag{4.1}$$

$$Z_0 = \begin{bmatrix} 0.25 & 0 & 0 & 0 \\ 0 & 0.4 & 0 & 0 \\ 0 & 0 & 0.2 & 0 \\ 0 & 0 & 0 & 0.01 \end{bmatrix}$$

$$Q = I_{4X4}$$

In spite of this deviation, CV2X-LOCA reliably beats other benchmark strategies beneath both lower and higher speed conditions, keeping up a Normal Localization Blunder (Lager) of less than 3 meters over all four street situations. These come about to highlight the strength of this work strategy in exploring complex urban situations and its ability to provide lane-level situating exactness over different activity scenarios.

We used LSE and LSE with Kalman filtering (LSE_KF) techniques in our research, with significant improvement in positioning precision over conventional techniques. While our theoretical approach is ideologically related to SDP-based techniques (like LSRE, SDP-, CV2X-LOCA, and SDP-ML-KF), our experimental implementation shows that even with the minimized LSE technique, we achieve superior performance in vehicle localization on diverse road environments. This observation agrees with the experimental findings of [41] and [42], which validates our conclusion that the principles behind our framework still hold with different mathematical implementations.

In [43] presented a localization algorithm based on vehicle-to-infrastructure (V2I), this algorithm is low-cost and needed hardware are simplified. Our method is more complicated and need hardware requirements more than algorithm in [43].

- Utilizing the LS process

The complete location error in case of LSE algorithm is < 9 m that is a large error as shown in Figure 4.4.

The x location error in case of LSE process is < 5 m as shown in Figure 4.5.

The y location error in case of using LSE process which is < 9 m as shown in Figure 4.6.

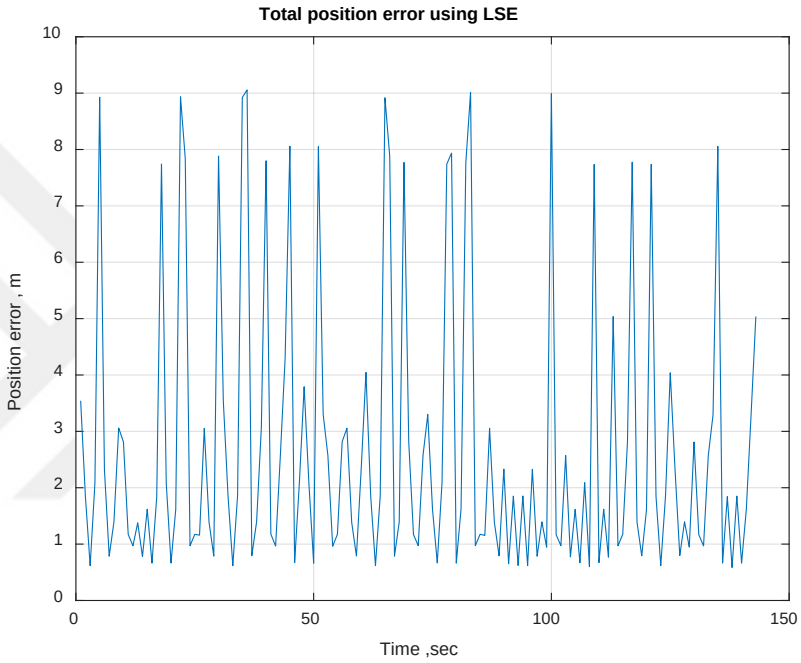


Figure 4.4. The complete location error utilizing LSE process.

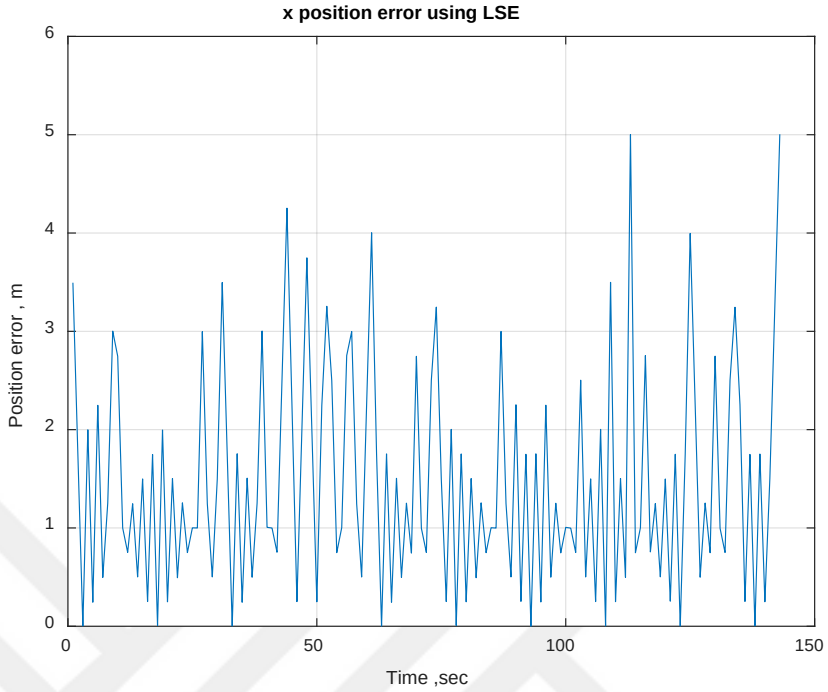


Figure 4.5. The x location error utilizing LSE process.

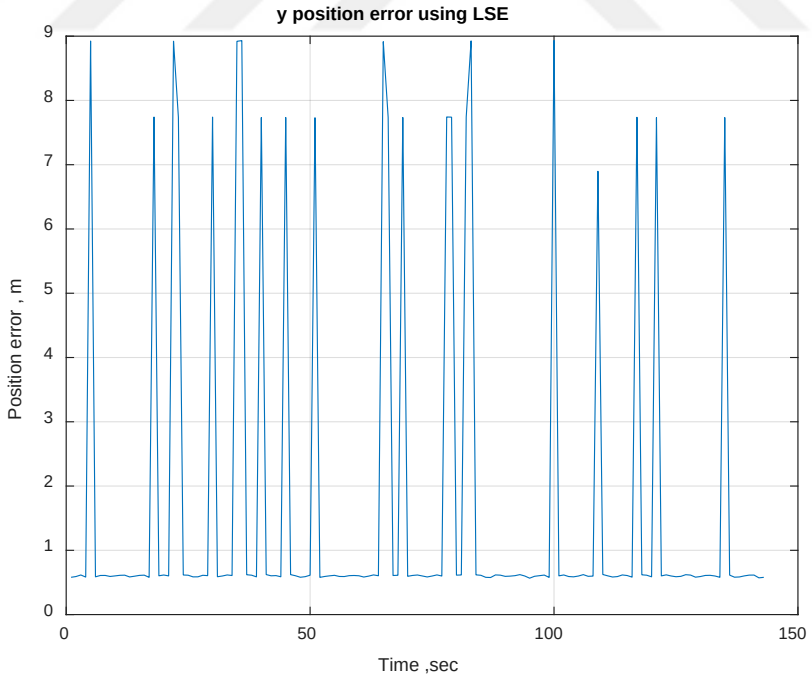


Figure 4.6. The y location error in case the LSE process.

- Utilizing Kalman filter process

  LSE Mae Error = 2.0 m.

  LSE Mape Error = 0.357m.

  LSE Mean Error = 1.76m.

  Figure 5.7 displays the all-location error utilizing LSE_KF process that is < 3 m.

  Figure 5.8 displays the x location error utilizing LSE_KF process that is < 2 m.

  Figure 5.9 displays the y location error utilizing LSE_KF process that is < 3 m.

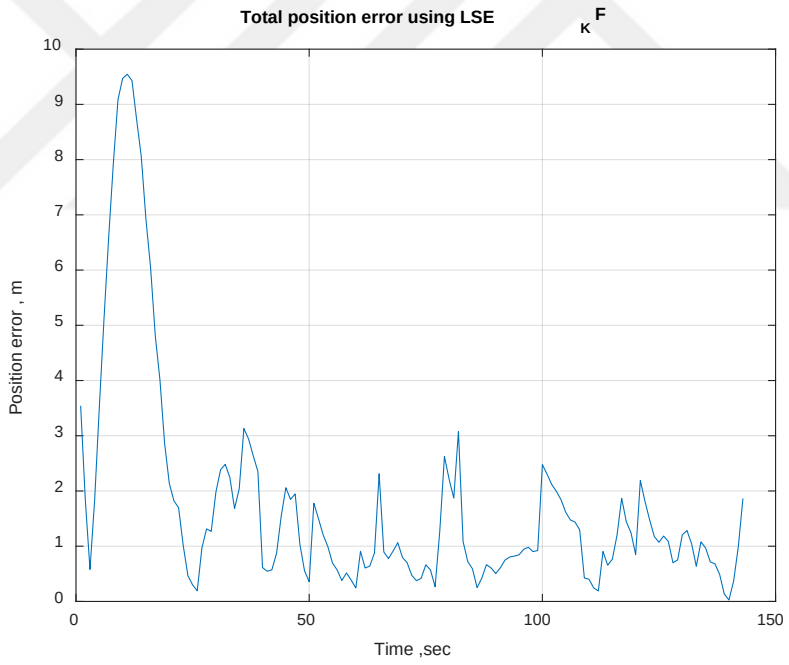


Figure 4.7. The total location error utilizing LSE_KF process.

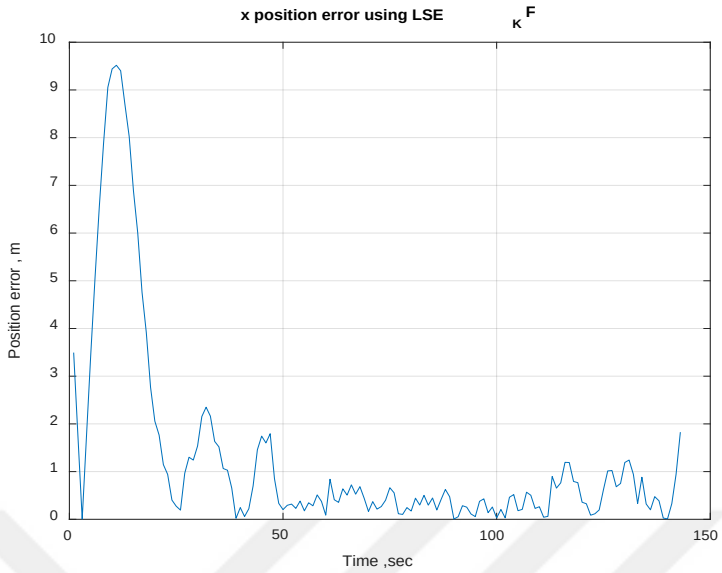


Figure 4.8. The x location error utilizing LSE_KF process.

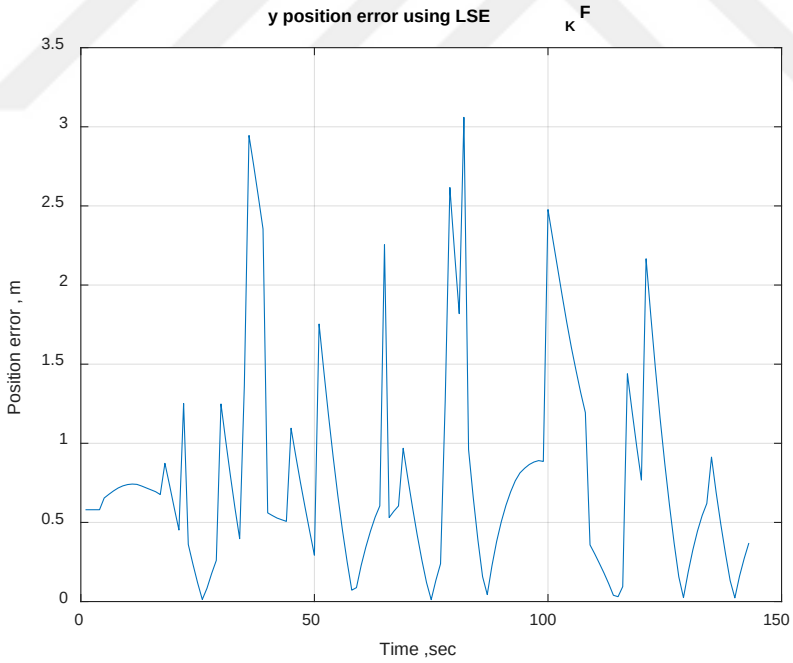


Figure 4.9. The y location error utilizing LSE_KF process.

The (MAPE, MAE, MEAN) errors in collected in the next table utilizing the LSE, LSE_KF process.

TABLE 4.2: The simulation errors (MAE, MAPE, MEAN).

| Error type | LSE Process | LSE_KF |
|---|---|---|
| Mae | 321.15 cm | 207.35 cm |
| Mape | 73.22cm | 35.65 cm |
| Mean | 271.02cm | 175.91 cm |

By utilizing the KF to approximate the error in the vehicle's position, the error in was decreased, as presented in Table 4.2**.**

[44] have used the nonlinear optimization solution method of the least-squares process and combined relative DOA and relative RD measurement, have determined the destination CAV's position value is determined with a precision of 3–4 m. In the present work by utilizing EKF the destination CAV's position value is determined to a proximity of 1-2.5 m.

Table 4.3: Comparison of our work and some related work:

| **Aspect** | **Our algorithm** | [7] | [8] | [9] | [10] | [11] | [12] |
|---|---|---|---|---|---|---|---|
| **Focus** | Roadside Unit-enabled cooperative localization for C-V2X autonomous vehicles | RSU-based cooperative localization using C-V2X | Comprehensive review of V2X communication, sensors, and AI for road safety | Feasibility and performance of C-V2X sensing-communication integration | Multi-modal fusion of image and RF signals for vehicle positioning | Intersection-specific positioning with UWB and onboard sensors | Deep learning-enhanced cooperative LiDAR sensing for vehicle positioning |
| **Technology** | C-V2X, RSU, and data fusion | C-V2X, RSU, and cooperative data fusion | V2X technologies, including sensors, communication, and AI | C-V2X combined with sensing systems | Image sensors, RF signals, AI | UWB sensors and onboard vehicle sensors | Cooperative LiDAR sensing and deep learning |

| **Aspect** | **Our algorithm** | [7] | [8] | [9] | [10] | [11] | [12] |
|---|---|---|---|---|---|---|---|
| **Contribution** | Proposed a cooperative localization framework to reduce position errors via RSU support | Demonstrated the benefits of RSU-assisted localization in reducing errors | Surveyed the field, analyzing the integration of various V2X-related technologies | Explored the feasibility of combining C-V2X sensing and communication | Improved localization accuracy using data fusion from multiple modalities | Fusion strategy for high-accuracy positioning in intersections | Proposed deep learning to enhance cooperative sensing among vehicles |
| **Novelty** | Integration of RSU with vehicle localization for high accuracy | Emphasized RSU's role in urban localization challenges | Broad overview without introducing a specific technical framework | Integrated sensing-communication design | Synergized RF and visual data for better vehicle positioning | Targeted intersection-specific localization | Machine learning for cooperative LiDAR accuracy improvement |
| **Application** | Urban and complex driving environments | General autonomous vehicle environments | Road safety and situational awareness | Diverse autonomous driving scenarios | Scenarios with occlusions or degraded sensor environments | Urban intersections and dense traffic | Cooperative environments with LiDAR-equipped vehicles |
| **Key Metrics** | Position error reduction, RSU communication efficiency | Localization error margins, scalability | No direct metrics; focused on technological state of the art | Signal processing latency, communication efficiency | Localization accuracy improvement | Position accuracy in high-traffic scenarios | Accuracy gains with minimal computational overhead |
| **AI Integration** | Not explicitly emphasized | Limited focus on AI | Significant focus on AI in review | Not explicitly emphasized | Central role in RF and image fusion | Limited application of AI | Core to the proposed deep learning framework |
| **Strengths** | Practical integration of RSU in localization; high compatibility with existing C-V2X systems | Scalability and real-world applicability of RSU-based systems | Comprehensive review; serves as a starting point for researchers | High potential for integration into existing systems | Robust in occluded or complex sensor environments | High precision in unique intersection challenges | Superior accuracy through cooperative learning |
| **Limitations** | Dependent on RSU deployment density | Requires extensive RSU infrastructure | Does not introduce new technologies; primarily a literature review | Limited focus on specific challenges, e.g., urban scenarios | Complex multi-modal system may require high computational resources | limited application, focused on intersections | Relies on LiDAR; may have limited generalization to non-LiDAR environments |

# 5. CONCLUSION and FUTURE WORK

This study introduces RSU-enabled cooperative localization framework, termed CV2X-LOCA, which relies on C-V2X channel state information. Its aim is to enable AVs to reach lane-level locating precision in GNSS-denied environments. The simulations have validated that CV2X-LOCA can attain high localization performance and maintain robustness across diverse road conditions, RSU deployment configurations, and communication scenarios. Consequently, this framework emerges as a viable option for AVs to attain lane-level global locating precision in the nonappearance of GNSS waves.

The proposed framework eliminates the need for on-board perception sensors in vehicles, thereby potentially reducing the operational and design costs associated with AVs. Furthermore, insights gleaned from the research on the optimal connectivity range could be beneficial to transportation authorities. This includes determining the RSU spacing for vehicle-to-infrastructure communication to minimize network topology fluctuations and identifying cost-effective strategies for RSU deployment to improve AV operations.

The potential impact of the shadowing effect on communication signals caused by obstructing line of sight (LOS) objects, such as trucks on the road, warrant consideration. Notably, the proposed framework could be seamlessly integrated with existing GNSS/INS systems, as well as onboard perception sensors and map data, to enhance locating accuracy. Consequently, future efforts will concentrate on extending the CV2X-LOCA framework to integrate with map data or on-board perception sensors to further refine locating accuracy.

. To finalize the study, it would be necessary to implement and test the proposed technique on actual settings, but this is outside the scope of the present work.

# REFERENCES


[1] G. e. a. Huang, ""Improved intelligent vehicle self-localization with integration of sparse visual map and high-speed pavement visual odometry."," *Automobile Engineering*, pp. 177-187, (2021).

[2] Y. e. a. Zhang, "Localization and tracking of an indoor autonomous vehicle depending on the phase difference of passive UHF RFID signals," 2021.

[3] Z. Z. M. e. a. Kassas, "Robust vehicular localization and map matching in urban environments through IMU, GNSS, and cellular signals," *Intelligent Transportation Systems Magazine*, pp. 36-52, 2020.

[4] Y. L. S. a. Y. Z. Alkendi, "State of the art in vision-depending localization techniques for autonomous navigation systems," pp. 76847-76874, 2021.

[5] P. A. A. Georgiev, "Localization methods for a mobile robot in urban environments," *IEEE Transactions on Robotics*, pp. 851 - 864, 2004.

[6] T. e. a. Nguyen, "Vision-depending multi-MAV localization with anonymous relative measurements using coupled probabilistic data association filter," *IEEE International Conference on Robotics and Automation (ICRA)*, 2020.

[7] Z. e. a. Huang, "Toward C-V2X Enabled Connected Transportation System: RSU-Based Cooperative Localization Framework for Autonomous Vehicles," *IEEE Transactions on Intelligent Transportation Systems* , 2024.

[8] S. A. A. K. a. R. S. Yusuf, "Vehicle-to-everything (V2X) in the autonomous vehicles domain–A technical review of communication, sensor, and AI technologies for road user safety," *Transportation Research Interdisciplinary Perspectives 23* , 2024.

[9] Y. e. a. Li, "Cellular V2X-based integrated sensing and communication system: Feasibility and performance analysis," *Chinese Journal of Electronics* , pp. 1104-1116, 2024.

[10] O. T. L. a. M. C. Huan, "Multi-modal Image and Radio Frequency Fusion for Optimizing Vehicle Positioning," *IEEE Transactions on Mobile Computing*, 2024.

[11] H. X. L. a. X. S. Gao, "A fusion strategy for vehicle positioning at intersections utilizing UWB and onboard sensors," 2024.

[12] L. e. a. Barbieri, "Deep Learning-based Cooperative LiDAR Sensing for Improved Vehicle Positioning," *IEEE Transactions on Signal Processing*, 2024.

[13] Z. Xiong, "Research on application of GPS-depending wireless communication system in highway landslide," *Wireless Communications and Networking*, p. 163, 2021.

[14] I. a. I. C. Zakharenkova, "Effects of storm-induced equatorial plasma bubbles on GPS-depending kinematic locating at equatorial and middle latitudes through the September 7–8, 2017, geomagnetic storm," p. 132, 2021.

[15] T. G. K. M. C. S. S. &. R. Omar, "Smart Cities V2I Cloud depending Infrastructure using Road Side Units," pp. 270-277, 2021.

[16] C.-H. Ou, "A roadside unit-depending localization scheme for vehicular ad hoc networks," *Communication Systems*, p. 135–150, 2014.

[17] Y. W. J. X. a. Y. X. L. Sun, "An RSU-assisted localization method in non-GPS highway traffic with dead reckoning and V2R communications," pp. 149-152, 2014.

[18] A. K. a. Y. A. F. A. A. Wahab, "Two-way TOA with limited dead reckoning for GPS-free vehicle localization using single RSU," p. 244–249, 2013.

[19] S. K. a. R. S. Parveen, "GPS-free localization in vehicular networks using directional antennas," *Data Engineering for Smart Systems*, 2022.

[20] A. a. F. D. Memedi, "A location-aware cross-layer MAC protocol for vehicular visible light communications," *Mobility, Sensing and Networking (MSN)*, 2021.

[21] O. Nabil, "Intervehicle-Communication-Assisted Localization," *IEEE Transactions on Intelligent Transportation Systems*, pp. 678 - 691, 2010.

[22] G. e. a. Yuan, "MIAKF: Motion inertia estimated adaptive Kalman filtering for underground mine tunnel positioning," *Instrumentation and Measurement*, 2023.

[23] R. P. a. S. Valaee, "Vehicular node localization using received-signal-strength indicator," *IEEE Transactions on Vehicular Technology*, p. 3371–3380, 2007.

[24] M. X. P. a. S.-W. Seo, "King's graph-depending neighborvehicle mapping framework," *Transactions on Intelligent Transportation Systems*, p. 1313–1330, 2013.

[25] G. e. a. Wan, "Robust and precise vehicle localization depending on multi-sensor fusion in diverse city scenes," *IEEE(ICRA)*, 2018.

[26] G. e. a. Huang, "Improved intelligent vehicle self-localization with integration of sparse visual map and high-speed pavement visual odometry," *Automobile Engineering*, pp. 177-187, 2021.

[27] C.-H. B.-Y. W. a. L. C. Ou, "GPS-free vehicular localization system using roadside units with directional antennas," *Communications and Networks*, pp. 12-24, 2019.

[28] S. B. a. L. Vandenberghe, "Convex Optimization," *Cambridge University Press*, 2004.

[29] P. Patil and A. Gokhale, "Improving the Reliability and Availability of Vehicular Communications Using Voronoi Diagram-Based Placement of Road Side Units," in *IEEE 31st Symposium on Reliable Distributed Systems*, Irvine, CA, USA, 2012.

[30] C. Ghorai and I. Banerjee, "A constrained Delaunay Triangulation based RSUs deployment strategy to cover a convex region with obstacles for maximizing communications probability between V2I," *Vehicular Communications*, pp. 89-103, 2018.

[31] A. Y. A. F. a. A. A. W. Khattab, "High accuracy GPS-free vehicle localization framework via an INS-assisted single RSU," *International Journal of Distributed Sensor Networks*, p. 795036, 2015.

[32] A. A. A. K. a. Y. A. F. Wahab, "Two-way TOA with limited dead reckoning for GPS-free vehicle localization using single RSU," *ITS telecommunications*, 2013.

[33] A. a. H. D. Matin, "Impacts of connected and automated vehicles on road safety and efficiency: A systematic literature review," *Transactions on Intelligent Transportation Systems*, pp. 2705-2736, 2022.

[34] F. P. G. a. C. W. Eckermann, "Cooperative Validation of CAM Position Information Using C-V2X," *Vehicular Technology*, 2020.

[35] Z. e. a. Huang, "Cv2x-loca: Roadside unit-enabled cooperative localization framework for autonomous vehicles," 2023.

[36] P. e. a. Li, "How Does C-V2X Perform in Urban Environments? Results From Real-World Experiments on Urban Arterials," *Transactions on Intelligent Vehicles* , 2023.

[37] E. S. A. A. a. D. B. H. Ma, "Radar image-based positioning for usv under gps denial environment," pp. 72-80, 2017.

[38] S. R. Jondhale and R. S. Deshpande, "Kalman Filtering Framework-Based Real Time Target Tracking in Wireless Sensor Networks Using Generalized Regression Neural Networks," *IEEE Sensors Journal*, pp. 224 - 233, 2018.

[39] J. G. H. Z. a. T. Z. Q. J. Li, "Rse-assisted lane-level positioning method for a connected vehicle environment," *IEEE Trans. Intell. Transp. Syst*, pp. 2644-2656, 2018.

[40] Y. P. a. W. Z. H. Qin, "Vehicles on rfid: Error-cognitive vehicle localization in gps-less environments," p. 9943–9957, 2017.

[41] J. I. a. G. J. K. Kim, "Tunnel facility based vehicle localization in highway tunnel using 3d lidar," p. 17 575–17 583, 2022.

[42] F. V. F. D. l. T. a. V. P. S. Panev, "Road curb detection and localization with monocular forward-view vehicle camera," pp. 3568-3584, 2018.

[43] Y. W. I. W.-H. H. W. S. a. L. C. Y. Wang, "Pavement marking incorporated with binary code for accurate localization of autonomous vehicles," p. 22 290–22 300, 2022.

[44] L. X. X. J. G. Y. Y. L. Faan Wang, "A Cooperative Positioning Method of Connected and Automated Vehicles with Direction-of-Arrival and Relative Distance Fusion," *mathematical problems in Engineering*, pp. 1-11, 2022.

[45] A. L. B. R. J. &. G. Haigermoser, " Road and track irregularities: measurement, assessment and simulation," *Vehicle System Dynamics*, pp. 878-957, 2015.